PHOTO-RESPONSIVE MICROCAPSULE SYSTEMS VIA SUPRAMOLECULAR CHEMISTRY

by

Kader Merve Türksoy

B.S., Chemistry, Kırıkkale University, 2007

Submitted to the Institute for Graduate Studies in
Science and Engineering in partial fulfillment of
the requirements for the degree of
Master of Science

Graduate Program in Chemistry

Boğaziçi University

2011

To My Family

ACKNOWLEDGEMENT

I would like to thank my supervisor Assoc. Prof. Amitav Sanyal for all his help and all those brain storming sessions we had together. It was absolutely invaluable. I gained different points of views not only in terms of chemistry but also in life experience and friendships during 2 years in Sanyal lab as a master student.

I would like to thank Assist. Prof. Rana Sanyal and Assist. Prof. Şenol Mutlu for giving their valuable time being my jury thesis.

I would like to thank Assist. Prof. Şenol Mutlu for his support on the use of Optical Microscope and also Burcu Selen Çağlayan and Ayla Türkekul for running my NMRs.

More thanks go to my dear lab family, especially, in no particular order, Oyuntuya Munkhbat, Gülen Yeşilbağ Tonga, Serap Yapar, Sezin Yiğit, Nergis Cengiz, Sebla Onbulak, Duygu Çıtak, Özgül Gök, Tuğçe Gevrek and Ece Manavoğlu who provided inspiration. Above all, many thanks to my friends who have made me the decision to apply Boğaziçi University and continue in master. They are Esin Soy, Cem Çelik and Alican Aktaş.

Finally, To my mother and oldest sister, I gratefully dedicate this thesis. Thank you for always supporting me. I think it was worth it.

ABSTRACT

PHOTO-RESPONSIVE MICROCAPSULE SYSTEMS VIA SUPRAMOLECULAR CHEMISTRY

Supramolecular self-assembly is a reversible process by which nanoparticles or other components spontaneously ordered into well organized functional structures due to their specific noncovalent interactions through their environment. These noncovalent interactions let the nano/micro-particles recognize each other and form different constructions such as micelles, microspheres, interface (membrane) or collodidal microcapsules. However, the construction of these systems requires a high degree of control to direct the nanoparticles' aggregation process. This thesis focuses on the formation and stabilization of self-assembled microcapsules that are obtained with noncovalent crosslinking interactions with an emphasis on photo-reversible ability of them. In this study, cyclodextrin functionalized gold nanoparticles and different photoswitchable crosslinker molecules were synthesized to obtain stimuli responsive colloidal microcapsules. Host-guest complexation between azobenzene molecule on the linker and cyclodextrin ligand on the nanoparticle surfaces leads to crosslinking of nanoparticles at the interface of water/organic-solvent emulsion. Resulting microcapsules were characterized using a variety of techniques such as optical microscopy, UV-Vis spectrometry and transmission electron microscope (TEM).

ÖZET

SUPRAMOLEKÜLER KİMYA YOLUYLA KURULAN IŞIL AYRILABİLİR MİKROKAPSÜLLER

Supramoleküler olarak kendiliğinden birleşme, nanopartiküllerin ya da diğer bileşenlerin çevreleri vasıtasıyla yapmış oldukları kovalent olmayan belirli etkileşimler sayesinde daha iyi organize olmuş işlevsel malzemeler olarak kendiliğinden düzenlenmelerini sağlayan tersinir bir yöntemdir. Kovalent olmayan bu etkileşimler nano/mikro-partiküllerin birbirlerini tanımasına ve misel, mikroküre, membran ya da koloidal mikrokapsüller gibi değişik yapılar oluşturmalarına izin verir. Fakat, bu sistemlerin oluşumu nanopartikül kümelenmelerine yön verebilecek yüksek seviyede bir kontrol gerektirir. Bu tez, ışıl yolla dönüşebilir yeteneği vurgulanarak, kovalent olmayan çapraz bağlama etkileşimleri sayesinde kendiliğinden bir araya gelen mikrokapsüllerin oluşumu ve stabilizasyonu üzerine durmaktadır. Bu çalışmada, uyaranlara tepki verebilen mikrokapsüller oluşturmak üzere siklodekstrin kaplı altın nanoparçacıklar ve ışıl yolla dönüşebilir birbirinden farklı çapraz bağlayıcı moleküller sentezlendi. Bağlayıcı üzerindeki azobenzen molekülü ve nanopartikül yüzeyi üzerindeki siklodekstrin ligandı arasındaki konuk-konak kompleksleşmesi su/organik-solvent emülsiyonu arayüzeyinde bir çapraz bağlama meydana getirir. Bu şekilde oluşan mikrokapsüller optik mikroskopi, UV-Vis spektrometri ve transmisyon elektron mikroskopi teknikleriyle gözlemlenmiştir.

TABLE OF CONTENTS

LIST OF FIGURES

LIST OF TABLES

LIST OF ACRONYMS/ABBREVIATIONS

AB	4-Phenylazobenzoicacid
AD	Adamantane
AP	4-Phenylazophenol
CD	Cyclodextrin
$CDCl_3$	Deutorated chloroform
CH_2Cl_2	Dichloromethane
DMAP	4-Dimethylaminopyridine
DMF	N,N-dimethylformamide
DMSO	N,N-Dimethyl sulfoxide
FTIR	Fourier Transform Infrared
MC	Microcapsule
MHz	Mega Hertz
NMR	Nuclear Magnetic Resonance
NP	Nanoparticle
TEA	Triethylamine
TEG	Tetraethylene glycol
THF	Tetrahydrofuran
UV	Ultraviolet

1. INTRODUCTION

1.1. Supramolecular Chemistry

1.1.1. Molecular Self-Assembly

Molecular self-assembly is a kind of assembly that occurs spontaneously between various molecules via noncovalent intermolecular forces. The supramolecular self-assembly systems let molecules recognize each other and integrate themselves into each other. This integration is achieved via noncovalent interactions, so that the construction process of those well-defined molecular architectures is a dynamically reversible and controllable process.

As with the self-assembly in nature, many biological systems can control over the molecules to get ordered structures in living organisms, for example self-assembly of lipid bilayer membrane in cells [1] or DNA folding [2]. Lipid bilayer makes up the membranes of cells. Each lipid molecule has a charged end that likes to be in water and a neutral end which is similar to oil (Figure 1.1).

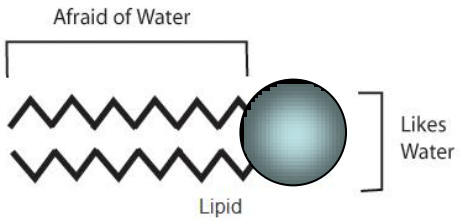

Figure 1.1. A simple illustration of a lipid molecule

Since the surroundings of cells are water, the lipids arrange themselves. Their oil-like parts hide themselves on inside and their water like parts turn to the outside that forms two layers of lipids, or a lipid bilayer (Figure 1.2).

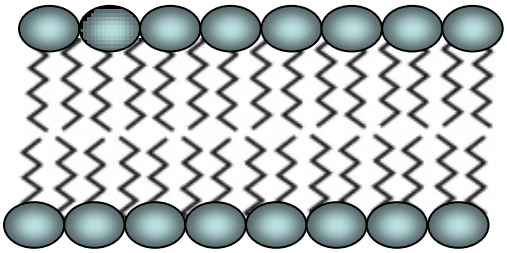

Figure 1.2. Lipid Bilayer, the oily parts hide on the inside of the cell membrane.

Similar to the nature, Scientists also make use of noncovalent hydrophobic interactions that provides molecules to self-assemble at the nanoscale for different properties. For this purpose they have created many interesting materials such as micelles [3], microspheres [4], vesicles [5], self-assembled monolayers (SAMs) [6] or colloidal microcapsules [7] via the noncovalent hydrophobic interactions (Figure 1.3).

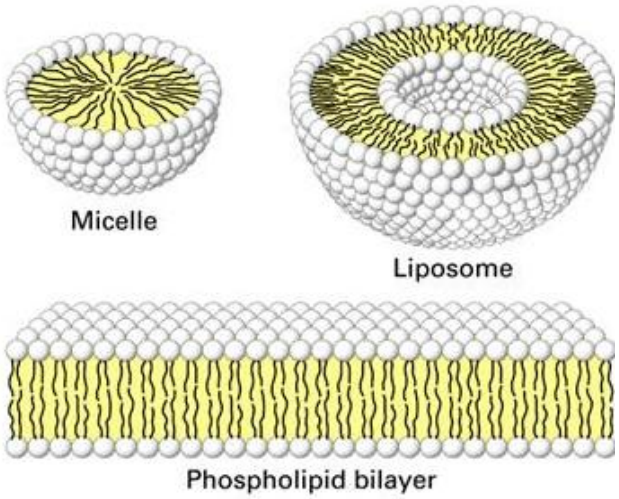

Figure 1.3. Similarity of noncovalent interactions between nature and science.

Molecular self-assembly defined as “the autonomous organization of components into patterns or structures without human intervention” [8], can be used for making assemblies of desired architectures from smaller molecules or building blocks. The interactions among the building blocks, subunits or the surroundings are exploited to bring nanoparticles order from disorder. Strenght of these nanoscale interactions can vary from a few kJ to hundereds of kJ. (Table 1.1) [9].

Table 1.1. Strenghts of Intermolecular Forces

Type Of Interaction	Strenght (kJ mol^{-1})
ion-ion	100-350
ion-dipole	50-200
dipole-dipole	5-50
hydrogen bonding	4-120
cation-π	5-80
π – π	0-50
van der waals forces	<5
metal ligand	0-400
covalent bonding	100-400
hydrophobic effects	difficult to assess

Self-assembly process has arisen a new area of chemistry called “supramolecular chemistry” [10]; that investigates molecular systems and the behavour of the nanoparticles or other components through intermolecular forces. By means of reversible noncovalent interactions, effective building blocks create great materials as multifunctional scaffolds for physical, chemical, and biological applications.

1.1.2. Molecular Recognition or Host-Guest Chemistry

In supramolecular chemistry, there are many important concepts one of which is molecular recognition that plays role on the construction of supramolecular systems. The molecular recognition, in another term; “Host-Guest Chemistry”, is the complementarity between the pairs , namely “host” and “guest” building blocks (Figure 1.4). According to the “host” and “guest” principle, the size, shape and position of the binding sites on a host are ideal for specific binding of the guest (e.g. substrate). This concept is the basis of the design and fabrication of different architectures.

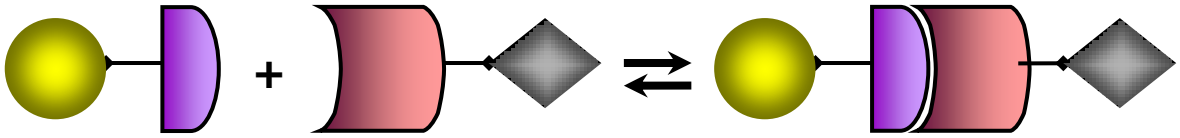

Figure 1.4. Reversible host-guest interaction via noncovalent forces.

Molecular recognition focuses on the basis of noncovalent forces which let molecules recognize each other. Such interactions for the nano-scale self-assembly may be hydrogen bonding, van der waals forces, pi-pi interactions, hydrophobic forces, electrostic effects or metal coordination etc. (Table 1.1).

1.1.3. Building Blocks of Supramolecular Chemistry

Supramolecular systems are created from well-defined structures or building blocks that they have ability to use to design larger functional architectures. Most of them exist as families of similar subunits, from which the structure with the desired properties can be chosen. The building blocks can be subdivided into different topics as shown in Table 1.2.

Table 1.2. Building Blocks of Supramolecular Chemistry.

Type of building block	Example
Synthetic Recognition Motifs	Crown ether, Porphyrins, etc.
Macrocycles	Cyclodextrins, Calixarenes, etc.
Structural Units	Nanoparticles, Dendrimers, Nanorods, etc.
Photo-/electro-chemically active units	Azobenzenes, Fullerenes, etc.
Biologically-derived units	DNA, Biotin, Enzymes, etc.

Supramolecular systems generally provide their suitable molecules to have appropriate spacing, and therefore easily-used structural units are required. As it is mentioned above, to achieve this strategy, host-guest chemistry was designed by scientists. Among all the building blocks which aim to use host-guest interaction, ‘cyclodextrin’, ‘adamantane’ and ‘azobenzene’ are of commonly used building blocks.

1.1.3.1. Cyclodextrins. Cyclodextrins are cyclic oligomers of glucose units joined by α-1,4-glucosidic linkages. Most common cyclodextrins are α, β, and γ cyclodextrins which have 6, 7 and 8 repeating units respectively (Figure 1.5). The hydrophobicity of their cavities help them make inclusion complexes with hydrophobic guest molecules in water media. Owing to their ability to form host-guest complexation they have been used in a number of industries such as pharmaceutical, food, cosmetic, tobacco and chemical industries [11-15]. In the chemical industry they have been used as catalysts, catalyst additives or separation media for some industrial products and for stabilization of azo dyes [16-17].

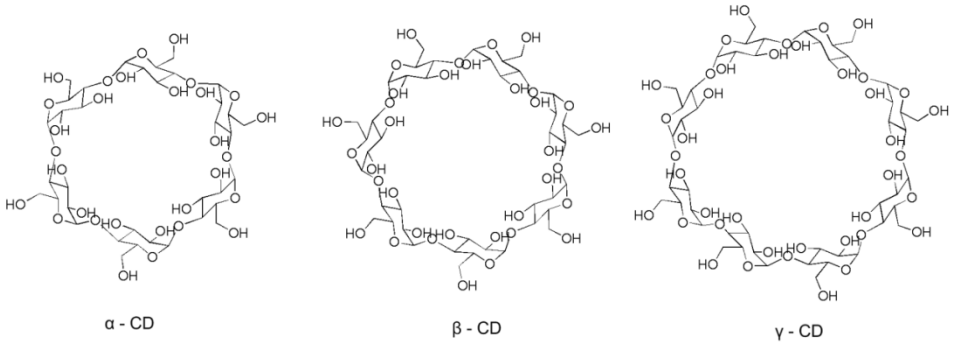

Figure 1.5. Cyclodextrins.

Hydrophobic forces between 'host' and 'guest' molecules depend on the hydrophobic cavity size of the host molecules. Upon selectivity on the cavity size, appropriate complexation occurs. For example, while adamantane molecule is a suitable guest for β-cyclodextrin [7] (Figure 1.13), azobenzene unit is able to fit into α-cyclodextrin (Figure 1.6) [18-19].

1.1.3.2. Azobenzene. Azobenzene which is a successively used structure as a 'guest' molecule, is an azo compound composed of two phenyl rings linked by a N=N double bond. One of the most attractive property of azobenzene (and its derivatives) is the photoisomerization property of it. The two isomers of azobenzene, 'trans' and 'cis' isomer forms of it, can be switched to each other with particular wavelengths of light. Irradiation of azobenzene with UV light at about 365 nm leads to isomerization of the azobenzene molecule from trans to cis form [20]. This transformation can be observed as a band change in absorbance in the UV Spectrometer. At 365 nm the absoption band at around 347 nm decreases remarkably, and the band at around 430 nm increases slightly. Because it

is a reversible action, when irradiated by visible light, at about 450 nm the absorption increases again, which proves the photoisomerization effect of azobenzene which undergoes a change from cis to trans form (Figure 1.6). This kind of control of the transformation is very advantageous in terms of the application to reversible building blocks, such as molecular shuttles, motors, and information storage [21].

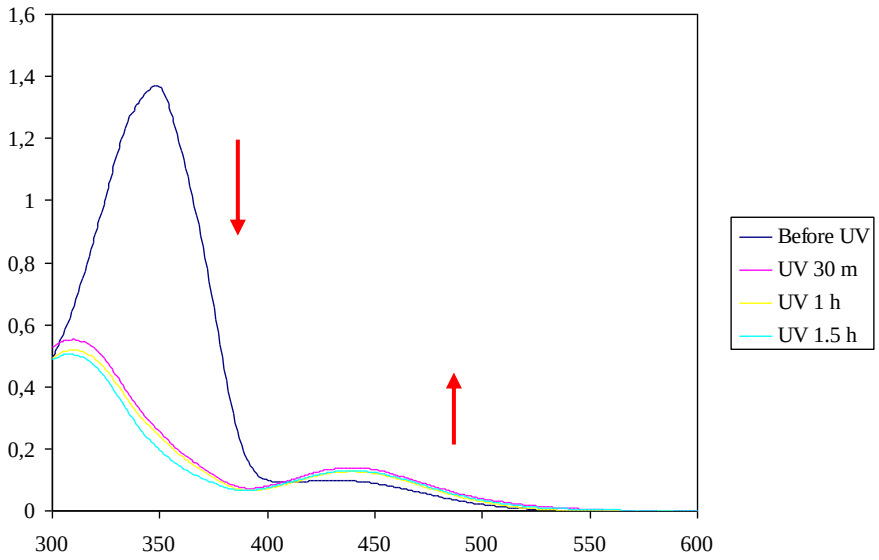

Figure 1.6. Absorption peak shift of 4-(phenylazo)benzoic acid under UV irradiation.

Reversible trans-cis isomerization of azobenzene unit can induce the inclusion and exclusion as a result of the stability of host-guest complexes [22]. Upon this photoreversible property of azobenzene, scientists created various complexes one of which was confirmed by Z. Wang and his coworkers. In their study, assembly of gold nanoparticles and multiwalled carbon nanotubes (MWNTs) with a switching function was successfully performed via photocontrolled host-guest interaction based on α-cyclodextrin (α-CD) and azobenzene derivatives (Figure 1.7).

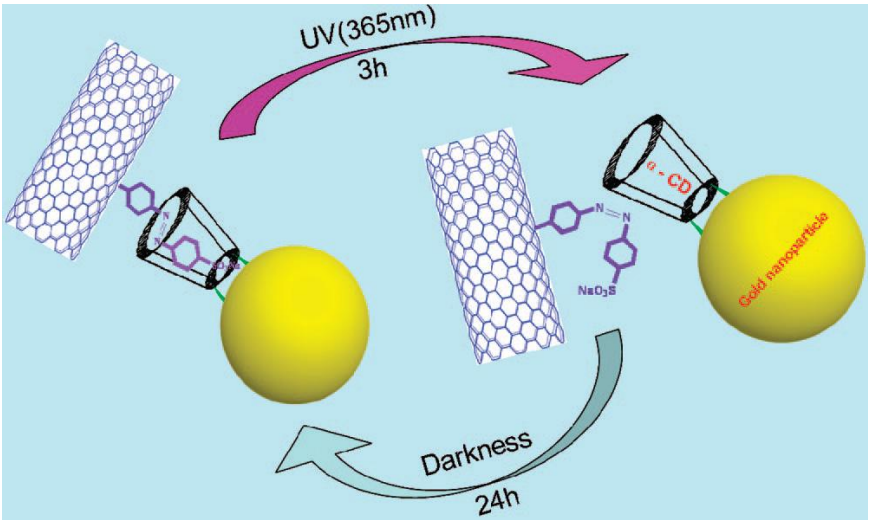

Figure 1.7. Schematic presentation of gold nanoparticles' reversible attachment onto and detachment from the surface of MWNTs through the photochemically controlled host-guest molecular recognition interaction.

The photo-chemically active control mechanism via host-guest interaction between azobenzene units on the surface of MWNTs and α –CD moieties on the gold nanoparticles has occured and the reversible interaction of gold nanoparticles onto the MWNT surface was confirmed. Using TEM images the photoreversible inclusion-exclusion complexation was demonstrated as the proof of the photoisomerization process (Figure 1.8) [23].

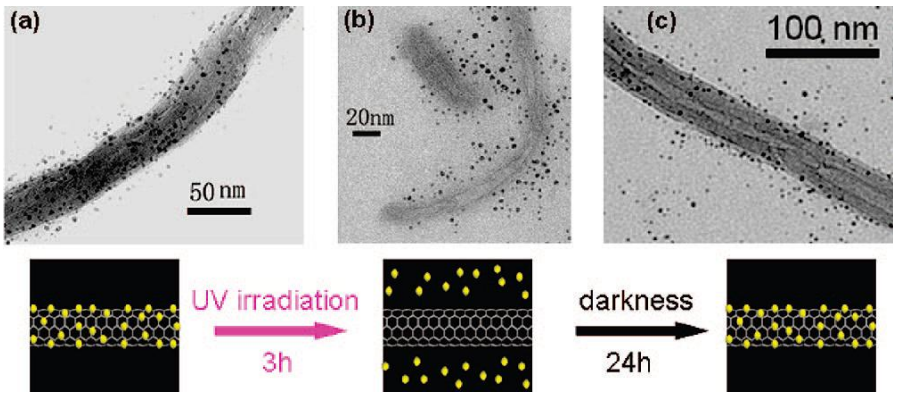

Figure 1.8. TEM images of the photocontrolled reversible attachment of AuNPs on modified MWNTs. (a) Mixing stoichiometric R-CD-capped AuNPs with MWNTs in water and stirring for 12 h, (b) UV irradiated for 3 h, and (c) standing for 24 h in the dark.

1.2. Microcapsules

Microcapsules, in another term “colloidosomes”, are small spherical shaped particles with a uniform surface around it where nanoparticles, such as gold or iron nanoparticles, are localized at and used as the building blocks of the intermolecular self-assembly. Colloidal microcapsules (MCs) are very well-organized and highly attractive materials due to their small size, high surface area, large inner volume and stable membrane formation at their surface. Owing to these properties, they have great potential as micro reactors as well as drug delivery and catalyst supports and encapsulants [24].

1.2.1. Building Blocks for Colloidal Microcapsules

Colloidal particles act as molecular building blocks and help incorporation of the particle properties into the functional abilities of the MCs. There are several types of nano- and microcapsules recently constructed, such as liposomes [25], polymerosomes [26,27] and polyelectrolyte capsules [28,29]. In terms of biology, the microcapsules have been clinically used for drug delivery, gene delivery and cancer treatment and other medical applications [30].

Nanoparticles can serve as appropriate antennae to show response to external triggers (e.g. magnetic fields or laser) for controlled release of encapsulated materials [31]. Also, the assembly of nanoparticles at liquid-liquid interfaces resulted in organized molecular structures [32] with unique electronic, magnetic and optical properties. These properties can be tuned by their size and interactions at both the macro- and nanoscopic level [33,34].

1.2.1.1. Gold Nanoparticles. Gold nanoparticles (Au NPs) are colloidal materials of metallic gold that are sub-micrometer-sized structures. Because of the mechanical effects at their range of size, their electronic, magnetic and optical properties are different from the properties of bulk metal. These properties based on size, distance, ligands and the shape of the particles [35].

The synthesis of gold nanoparticles includes two different methods. The first method is “citrate reduction“ used method by Turkevitch [36], $HAuCl_4$ is reduced by trisodium

citrate in aqueous media, while Brust-Schiffrin [37] method (Figure 1.9) obtains thiol stabilized gold nanoparticles by reduction of $HAuCl_4$ in the presence of $NaBH_4$.

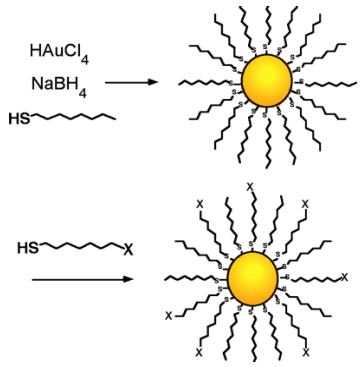

Figure 1.9. Synthesis of Au NPs via Brust-Schiffrin method.

As a result of their nature, NPs tend to aggreate and the ligand protection is needed to prevent the aggregation of the NPs. Ligands which have affinity to the surface of AuNPs are thiols, phosphine oxides, amines, phosphines and carboxylates. Among all thiols are mostly used ligands due to the stability of their self assembled monolayers on gold.

1.2.2. Stabilization of the Microcapsules

During the fabrication of microcapsules, colloidal nanoparticles tend to localize at the liquid-liquid interface to minimize the interfacial energy between two immiscible liquids, for example oil-water (o/w) emulsions (Figure 1.10).

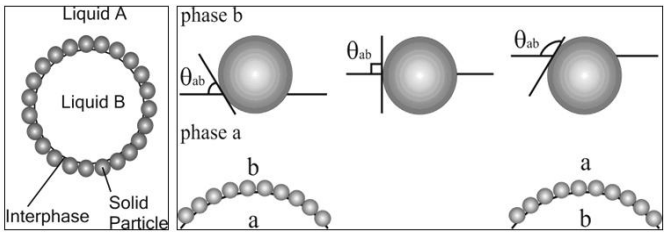

Figure 1.10. A single droplet stabilized by solid particles and influence of the contact angle on the emulsion.

The stabilization of colloidal particles was first observed almost a century ago and termed “Pickering emulsions”. Later Pieranski showed that the decrease in interfacial energy is directly proportional to the radius of nanoparticle and surface tension of the NP template with respect to ail (O) and water (W) according to the following equation [38]

$$\Delta E = - \frac{\pi r^2}{\gamma_{o/w}} \times [\gamma_{o/w} - (\gamma_{p/o} - \gamma_{p/w})]^2 \qquad (1.1)$$

where $\gamma_{o/w}$ is the oil/water interfacial tension, $\gamma_{p/o}$ is the particle/ail interfacial tension and $\gamma_{p/w}$ is the particle/water interfacial tension.

1.2.2.1. Effect of the Nanoparticle Radius (r). According to the equation (1,1), stabilization of the particle at the liquid–liquid interface is strongly size-dependent; ΔE is proportional to r^2, so the gained energy is smaller and the assembly is weaker when smaller NPs are used. While micron-sized particles irreversibly adsorb at the interface and make stable emulsions, nano-sized particles (<20 nm) adsorb more weakly at the interface. So, the thermal deviations cause the displacement of NPs from the interface and size-selective particle assembly occurs (Figure 1.11a).

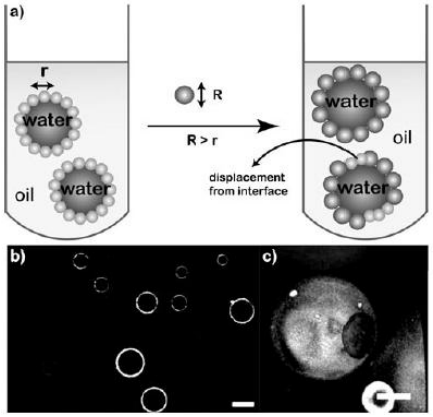

Figure 1.11. Schematic representation and confocal images of NPs. (a) Schematic of size selective displacement from interface. Confocal Microscopy images of (b) 2.8 nm CdSe stabilized droplets (c) Droplets after addition of 4.6 nm CdSe NPs. Scale bar, 20 μm.

Scientists gained access to size-selective adsorption of NPs at the oil–water interface by using fluorescent CdSe quantum dots [39]. Firstly, smaller green CdSe NPs were used to stabilize water-in-oil type emulsions. They then added larger red CdSe NPs to the toluene phase. As a result, larger CdSe NPs assembled on the surface of stabilized droplets and displaced the smaller NPs (Figure 1.11b).

1.2.2.2. Wettablity of Nanoparticles. Wettability is directed by three phase contact angle [40]. The relationship between contact angle and interfacial tensions can be derived by using Young's following equation

$$\cos\theta = \frac{\gamma_{p/o} - \gamma_{p/w}}{\gamma_{o/w}} \quad (1.2)$$

where θ = contact angle. The selectivity of NPs through the solvents is a significant determinant, as indicated by $\gamma_{p/o}$ and $\gamma_{p/w}$ in the above equation. Generally, hydrophilic NPs ($\gamma_{p/o} > \gamma_{p/w}$, θ <908) stabilize oil-in-water emulsions, while hydrophobic NPs ($\gamma_{p/o} < \gamma_{p/w}$, θ >908) are used to stabilize water-in-oil emulsions. Only particles with appropriate wettability ($\gamma_{p/o} = \gamma_{p/w}$, θ = 908) lead to stable emulsions.

1.2.2.3. Interparticle Interaction at Oil-Water Interface. Interfacial interactions between particles at the liquid–liquid interface play an impoartant role in the self-assembly process. In essence, interfacial forces such as capillary, solvation, electrostatic, van der Waals, and fluctuation forces are responsible for manipulating these interactions at the liquid-liquid interface of MCs [41].

1.2.3. Crosslinking of NPs at the Liquid–Liquid Interface

Crosslinking helps NPs form a stable 2D network structure at the emulsion interface, which leads to stable MCs. The easiest way of crosslinking NPs at the oil–water interface is to link their ligands through chemical bonds. The crosslinking can be subdivided into two topics; (i) covalent interactions between NPs, and (ii) noncovalent interactions between NPs.

1.2.3.1. Covalent Interaction Between Nanoparticles. Covalent crosslinking between ligands provides mechanical integrity and structural stability to the NP assemblies [42].

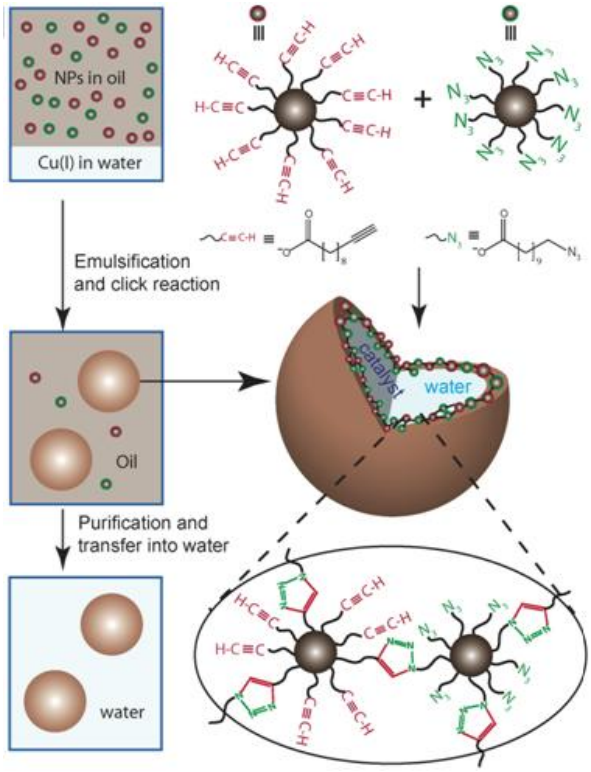

Figure 1.12. Formation of magnetic colloidosomes synthesis through self-assembly at water-in-oil interfaces followed by interfacial crosslinking of NPs via click chemistry and cross-sectional view of colloidosome.

As an example for covalent interaction between NPs, copper(I) catalyzed Huisgen-type [3+2] "click" cycloadditions were used for the crosslinking of NPs at the interface of water-in-oil emulsions. In this study, alkyne and azide-functionalized Fe_3O_4 NPs were brought together at the interface and covalently linked using the CuI catalyst present in the aqueous microdroplets (Figure 1.12) [43].

1.2.3.2. Noncovalent Interaction Between Nanoparticles. Molecular recognition provides a noncovalent coupling between complementary molecules or surfaces functionalized complementary molecules to create novel functional materials and molecular assemblies [44].

In a recent work, Sanyal and Rotello reported the fabrication of colloidal microcapsules through "host–guest" type molecular recognition at the liquid–liquid interface (Figure 1.13a) [7]. Water-soluble β-cyclodextrin-capped gold NPs and organo-soluble adamantylfunctionalized gold NPs were self-assembled at the water–toluene interface through specific host–guest molecular interactions to provide robust microcapsules. Multivalent interactions of the complementary ligands on the NPs surface provide stability to these capsules and no stabilization was observed when either NP was used alone.

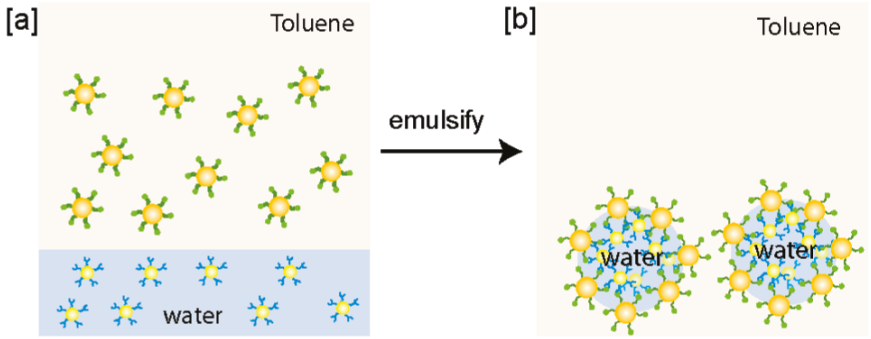

Figure 1.13. Fabrication of colloidal microcapsules. (a) NP1 and NP2 dispersed in water and toluene, respectively. (b) Fabrication of colloidal microcapsule via recognition mediated crosslinking.

2. AIM OF THE STUDY

The formation of stimuli-responsive colloidal microcapsules due to crosslinking via specific non-covalent ‘host-guest’ chemistry is a developing area. Unlike covalently cross-linked microcapsules, the reversible nature of these bridging noncovalent interactions is a challenging issue. As a novel alternative, we envisioned that photoreversible host-guest interaction between water soluble cyclodextrin functionalized gold nanoparticles and organo soluble photoswitchable crosslinker molecules could lead to crosslinking of nanoparticle at the interphase to afford stable and photoresponsive microcapsules.

Azobenzene is a light-responsive material that can be reversibly isomerized from trans to cis form under UV irradiation. Also, each water soluble cyclodextrin functionalized gold nanoparticle is a suitable ‘host’ for trans isomer form of hydrophobic azobenzene moiety due to the inclusion complexation between cyclodextrin and trans azobenzene. Cyclodextrin containing gold nanoparticles when mixed with homobifunctional noncovalent crosslinker, containing two azobenzene molecules in the binding sides, would result in the formation of photoreversible microcapsules due to the crosslinking of nanoparticles via specific noncovalent host-guest chemistry. After UV irradiation trans azobenzene turns into cis azobenzene and the cleavage of microcapsules occurs because of the mismatch between azobenzene and cyclodextrin.

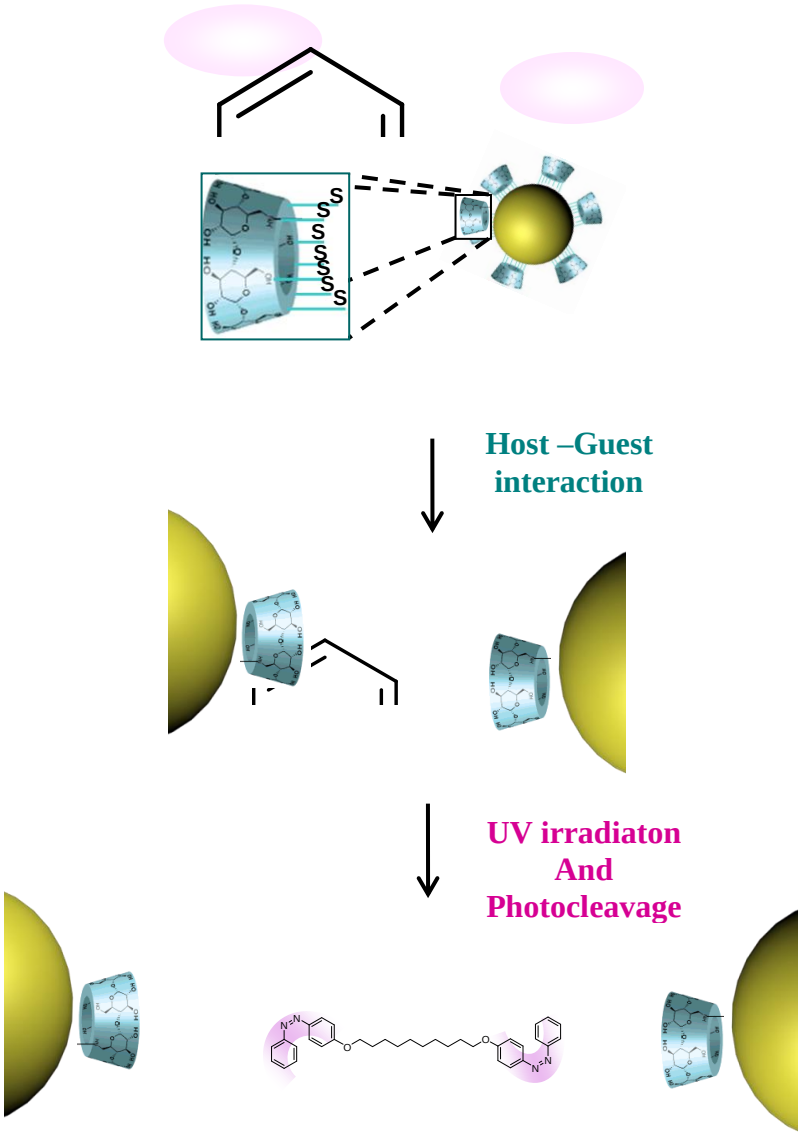

Figure 2.1. Schematic illustration of the aim of the study. Host-guest molecular interaction between CD functionalized Au NPs and azobenzene containing crosslinker molecule and the photocleavage of MCs after UV irraditon.

3. EXPERIMENTAL

3.1. Methods and Materials

All chemicals were reagent grade and were used as received from manufacturer (Merck, Aldrich, Alfa Aesar, and Riedel de Haen) unless otherwise noted. Dry CH_2Cl_2 was obtained from ScimatCo Purification System, dry DMF was dried of molecular sieves. Coloumn Chromatography was performed using silicagel-60 (43-60 nm). Thin layer chromatography was performed using silica gel plates (Kiesel gel F254, 0.2 mm, Merck). Plates were viewed under 254 nm UV lamp. Infrared Spectroscopy was carried out on Thermo Scientific Nicolet 380 FTIR spectrophotometer. ^{1}H NMR (operating at 400 MHz) and was recorded on Varian Mercury-MX in $CDCl_3$ as solvent at the Advanced Technologies Research and Development Center at Boğaziçi University.

3.2. Synthesis

3.2.1. Synthesis of β Cyclodextrin Functionalized Au Nanoparticles

3.2.1.1. Synthesis of Per iodo β Cyclodextrin. According to a literature procedure [45], to a solution of Ph_3P (6.91 g, 26.4 mmol) in dry DMF (30 mL), I_2 (6.98 g, 27.6 mmol) was added over 15 mins. Heat evolved during this addition and the solution increased in temperature from RT to approximately 50 °C. Dry β -cyclodextrin (2.00 g, 10.2 mmol) was then added to this dark brown solution and the temperature was raised to 70 °C using an oil bath. The solution was stirred at this temperature for 20 h. The heat was removed, and the solution was concentrated to 1/3 of its original volume. To this residue, NaOMe in MeOH (3.00 M, 10.3 mL) was added where the reaction was cooled in an ice/salt slurry and the mixture was stirred for 30 mins. The reaction mixture was then poured into MeOH (150 mL) to form a precipitate, which was then washed with MeOH 6-7 times by successive dispersions and centrifugations. ^{1}H NMR spectrum was in agreement with the literature data.

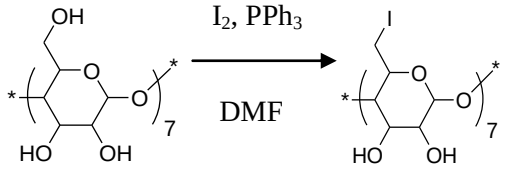

Figure 3.1. Synthesis of Per iodo β CD.

3.2.1.2. Synthesis of Per thio β –Cyclodextrin. According to a literature procedure [46], per iodo cyclodextrin (0.500 g, 0.26 mmol) was dissolved in DMF (6 mL); thiourea (0.156 g, 2.05 mmol) was then added and the reaction mixture heated to 70 ^{o}C under a nitrogen atmosphere. After 19 h, the DMF was removed under reduced pressure to give a yellow oil, which was dissolved in water (25 mL). Sodium hydroxide (0.135 g, 3.37 mmol) was added and the reaction mixture heated to a gentle reflux under a nitrogen atmosphere. After 1 h, the resulting suspension was acidified with aqueous $KHSO_4$ and the precipitate filtered off, washed thoroughly with distilled water, and dried. To remove the last traces of DMF, the product was suspended in water (25 mL) and the minimum amount of potassium hydroxide added to give a clear solution; the product was then reprecipitated by acidifying with aqueous $KHSO_4$. The resulting fine precipitate was carefully filtered off and dried in the freeze-drier. ^{1}H NMR spectrum was in agreement with the literature data.

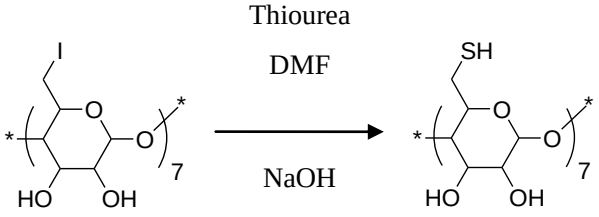

Figure 3.2. Synthesis of Per thio β CD.

3.2.1.3. Sythesis of β-Cyclodextrin Functionalized Au Nanoparticles. According to a literature procedure [47], $HAuCl_4$ (90 mg, 0.27 mmol) was dissolved in DMSO (10 mL). This solution was mixed quickly with a solution of $NaBH_4$ (123 mg, 3.25 mmol) and per thio cyclodextrin (100 mg, 0.08 mmol) in DMSO (10 mL). The reaction mixture turned deep-brown immediately, and was allowed to continue for 24 h. At this point, CH_3CN (20 mL) was added to precipitate the nanoparticles, which were collected and purified by

centrifugation, followed by washing with CH_3CN:DMSO (1:1 v/v, 30 mL) and ethanol (30 mL), dissolution in water, and freeze-drying. ^{1}H NMR spectrum was in agreement with the literature data.

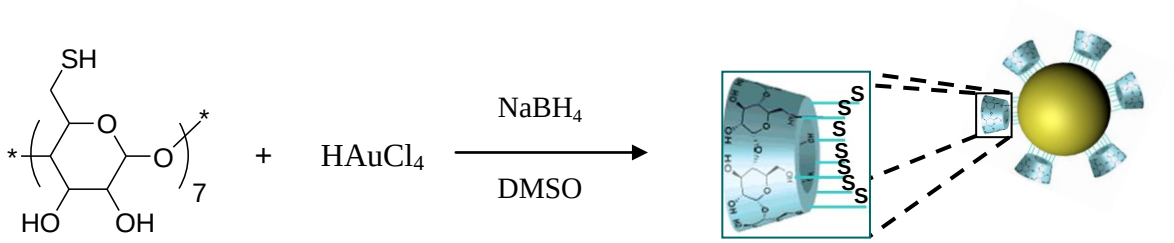

Figure 3.3. Synthesis of β CD Functionalized Au NPs.

3.2.2. Synthesis of α -Cyclodextrin Functionalized Au Nanoparticles

3.2.2.1. Synthesis of Per iodo α-Cyclodextrin (α -CD-I). As described in a previous article [48], α -CD (6.48 g, 6.66 mmol) was added to a stirred solution of triphenylphosphine (31.5 g, 120 mmol) and iodine (30.5 g, 120 mmol) and the solution was stirred at 80 ^{o}C for 15 h. It was then concentrated under vacuum to half of its volume and the pH was adjusted to 9–10 by the addition of sodium methoxide in MeOH (3.0 M, 45 mL) with simultaneous cooling. The solution was kept at room temperature for 30 min to destroy the formate esters formed in the reaction. It was then poured into 800 mL of MeOH to form precipitate, washed with MeOH and acetone successively. The resulting precipitate was dried superficially. Then α-CD-I was recovered as white powder. ^{1}H NMR spectrum was in agreement with the literature data.

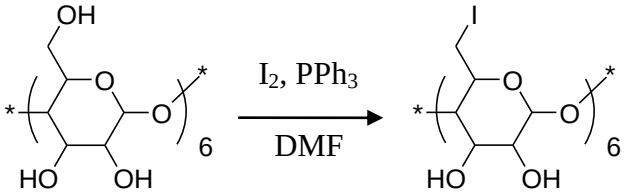

Figure 3.4. Synthesis of Per iodo α CD.

3.2.2.2. Synthesis of Per thio α –Cyclodextrin (α -CD-SH). According to a literature procedure [48], 6.71 g α -CD-I was dissolved in 40 mL of DMF and 2.118 g thiourea was then added. The reaction mixture was heated to 70 ^{o}C under a N_2 atmosphere. After 19 h,

DMF was removed under reduced pressure to give a yellow oil product, which was dissolved in 150 mL DDI water. 1.82 g NaOH was added and the reaction mixture was heated to a gentle reflux under a N_2 atmosphere. After 1 h, the resulting suspension was acidified with aqueous $KHSO_4$ and the precipitate was collected by centrifugation, washed thoroughly with DDI water, and dried. To remove the last traces of DMF, the product was suspended in 300 mL DDI water and a minimum amount of KOH was added to give a clear solution; the product was then re-precipitated by acidifying with aqueous $KHSO_4$. The resulting α -CD-SH fine precipitate was carefully centrifuged and dried. ^{1}H NMR spectrum was in agreement with the literature data.

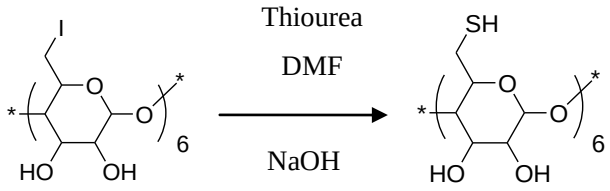

Figure 3.5. Synthesis of Per thio α CD.

3.2.2.3. Sythesis of α -Cyclodextrin Functionalized Au Nanoparticles. According to the literature procedure [49,51], $HAuCl_4$ (9 mg, 0.027 mmol) was dissolved in DMSO (2 mL). This solution was mixed with a solution of $NaBH_4$ (80 mg, 2.116 mmol) and per thio cyclodextrin (24.4 mg, 0.023 mmol) in DMSO (3 mL). The reaction mixture turned deep-brown immediately, and stirred for 24 h. At this point, CH_3CN (5 mL) was added to precipitate the nanoparticles, which were collected and purified by centrifugation, followed by washing with CH_3CN:DMSO (1:1 v/v, 10 mL) and ethanol (10 mL), dissolution in water, and freeze-drying. ^{1}H NMR spectrum was in agreement with the literature data.

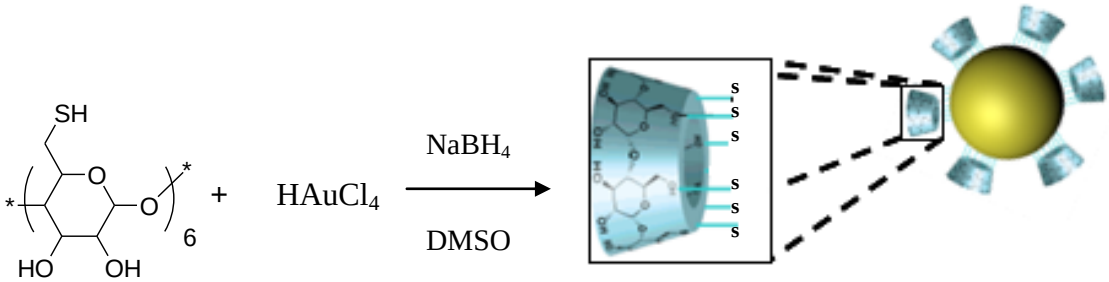

Figure 3.6. Synthesis of α CD Functionalized Au NPs.

3.2.3. Synthesis of the linker Adamantyl-(4-phenyl)azobenzoyl tetraethyleneglycol (AB-TEG-AD)

3.2.3.1. Synthesis of 4-phenylazobenzoylfluoride. According to a literature procedure [52], a suspension of 4-phenylazobenzoic acid (0.226 g, 1 mmol) and pyridine (0.162 mL, 2 mmol) in dry DCM (5 mL) was cooled to 0 °C under an argon atmosphere. To this was added cyanuric fluoride (0.172 mL, 2 mmol), and the contents were stirred for 90 min. A deep red/orange color was observed. Crushed ice/water (5 g) was then added, the suspension filtered, and the organic layer separated and washed with cold water (2 x 5 mL). Concentration in vacuo followed by chromatography (SiO_2, 6:1 Hex/EtOAc) provided 0.184 g (80%) of 4-phenylazobenzoylfluoride as a darkorange crystalline. ^{1}H NMR was as predicted in the agreement with the literature data.

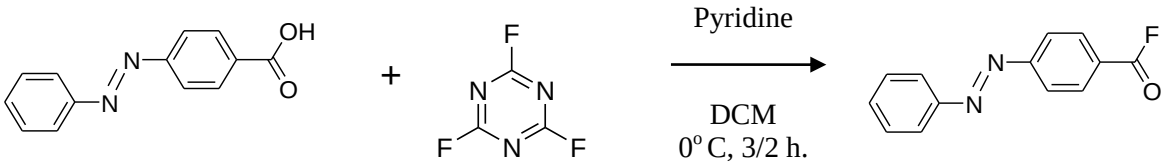

Figure 3.7. Synthesis of 4-phenylazobenzoylfluoride.

3.2.3.2. Synthesis of Adamantane Tetraethylene Glycol. Adamantane tetraethylene glycol was synthesized according to a lituretature procedure [53]. Adamantyl bromide (0.5 g, 2.32 mmol) was dissolved in tetraethylene glycol (TEG) **(**10 mL) and triethylamine (TEA) (98 µL, 6.52 mmol) added. The mixture was allowed to react for 48 h at 120 ^{o}C. The reaction mixture was diluted with 25 mL CH_2Cl_2 and extracted with 1M HCl (2 x 25 mL) and then H_2O (3 x 25 mL). The residue was dried over Na_2SO_4, filtered and volatiles evaporated under vacuum. The crude product was purified by column chromatography with ethyl acetate:hexane (80:20) to yield adamantyl tetraethylene glycol (AD-TEG) as yellow oil. ^{1}H NMR spectrum was in agreement with the literature data.

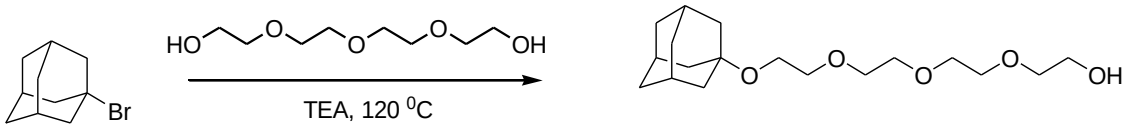

Figure 3.8. Synthesis of Adamantane tetraethylene glycol.

3.2.3.3. Synthesis of Adamantyl-(4-phenyl)azobenzoyl-Tetraethyleneglycol (AB-TEG-AD). 4-phenylazobenzoylfluoride (0.195 g, 0.8 mmol) solution in 8 mL dry DCM (is added to the suspension of AD-TEG (0.209 g, 0.64 mmol) and DMAP (0.077 g, 0.64 mmol) in 2 mL dry DCM. After stirring the solution for 24 h. at room temperature, it was extracted with H_2O (2x20 mL) and DCM (2X40 mL). The combined solution was dried with Na_2SO_4 and concentrated in vacuo. The crude product was purified by column chromatography with ethyl acetate:hexane (40:60) to yield the product as an orange solid. ^{1}H-NMR ($CDCl_3$, δ, ppm) = 8.23-8.21 (d, 2H), 7.96-7.94 (d, 4H), 7.54-7.52 (t, 3H), 4.52 (t, 2H), 3.87 (t, 2H), 3.71-3.70 (m, 4H), 3.62-3.61 (t, 2H), 3.60-3.57 (t, 2H), 2.51 (m, 3H), 1.72-1.69 (d, 6H), 1.63-1.54 (dd, 6H) (Figure A.1).

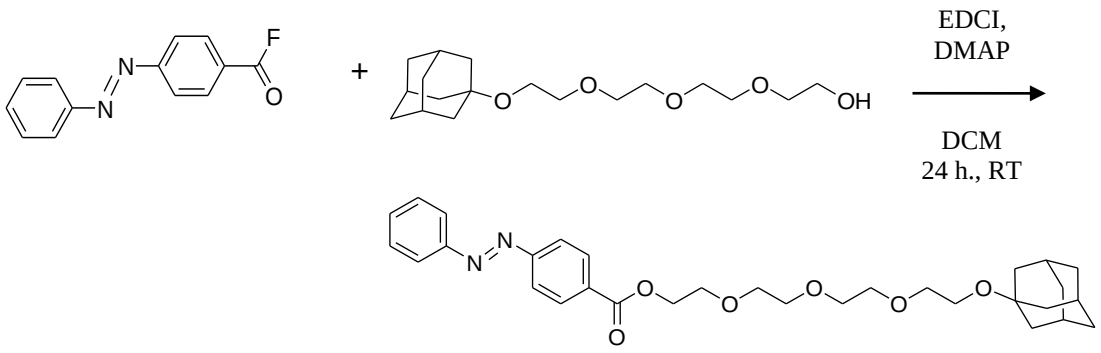

Figure 3.9. Synthesis of the linker AB-TEG-AD.

3.2.4. Synthesis of the linker 1-Adamantoyl-6-(4-phenylazo)benzoyl-Hexane (AB-Hex-AD)

3.2.4.1. Synthesis of Adamantoyl-Hexanol (AD-Hex-ol). The solution of Adamantane-1-carbonyl chloride **(**1.0 g, 5 mmol) and TEA (1.012 g, 10 mmol) in dry 30 mL DCM was added to the suspension of 1,6-Hexanediol (2.954 g, 25 mmol) and DMAP (0.305 g, 2,5

mmol) in 30 mL dry DCM. The mixture was allowed to react for 48 h at room temperature. The reaction mixture was extracted with 1M HCl (2 x 30 mL) and then H_2O (3 x 30 mL). The residue was dried over Na_2SO_4, filtered and volatiles evaporated under vacuum. The crude product was purified by column chromatography with ethyl acetate:hexane (10:90) to yield Adamantoyl-Hexanol (AD-Hex-ol). ^{1}H NMR spectrum ($CDCl_3$, δ, ppm) = 4.02 (t, 2H), 3.65-3.60 (q, 2H), 1.99 (m, 3H), 1.86-1.85 (d, 6H), 1.69 (t, 6H), 1.61-1.56 (m, 4H), 1.38-1.35 (p, 4H) (Figure A.3).

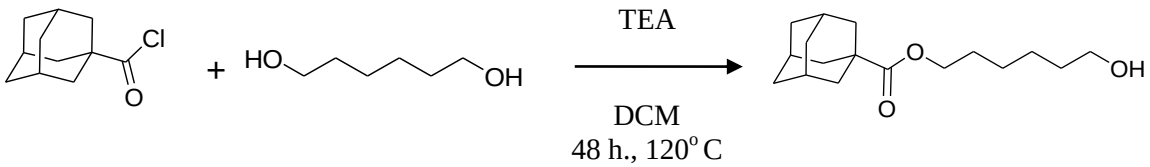

Figure 3.10. Synthesis of Adamantoyl-Hexanol.

3.2.4.2. Synthesis of 1-Adamantoyl-6-(4-phenyl)azobenzoyl-Hexane (AB-Hex-AD). The solution of 4-phenylazobenzoylfluoride (55 mg, 0.225 mmol) in 3 mL dry DCM was added to the suspension of 6-Adamantoyl-Hexanol (56.5 mg, 0.2 mmol) and DMAP (24.7 mg, 0.2 mmol) in 2 mL dry DCM. The mixture is stirred for 24 h. at room temperature. After stirring, it was extracted with H_2O (2x10 mL) and DCM (2x20 mL). The residue was dried over Na_2SO_4, filtered and volatiles evaporated under vacuum. The crude product was purified by column chromatography with ethyl acetate:hexane (10:90) to yield an orange solid product. ^{1}H-NMR ($CDCl_3$, δ, ppm) = 8.18-8.16 (d, 2H), 7.95-7.92 (d, 2H), 7.53-7.51 (d, 2H), 4.34 (t, 2H), 4.05 (t, 2H), 1.98 (m, 3H), 1.86 (d, 6H), 1.83-1.77 (p, 2H), 1.69 (m, 6H), 1.65-1.62 (p, 2H), 1.51-1.41 (m, 4H) (Figure A.5).

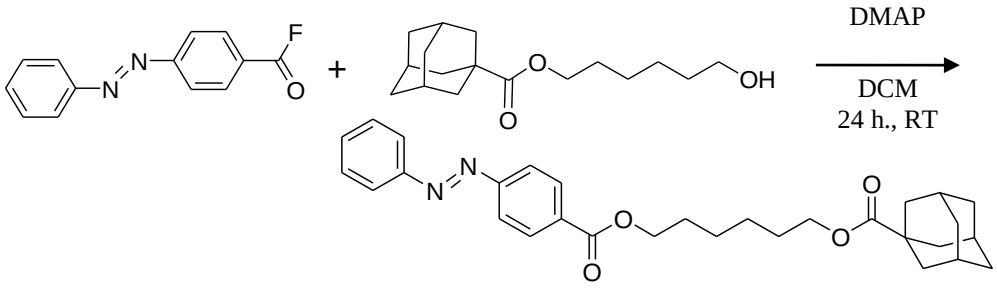

Figure 3.11. Synthesis of the linker AB-Hex-AD.

3.2.5. Synthesis of the linker 1,6-di(4-(phenyldiazenyl)benzoyl)-hexane (AB-Hex-AB)

3.2.5.1. Synthesis of 1,6-di(4-(phenyldiazenyl)benzoyl)-hexane. The solution of 4-phenylazobenzoylfluoride (367 mg, 1.50 mmol) in 6 mL dry DCM was added to the suspension of 1,6-Hexanediol (53 mg, 0.45 mmol) and DMAP (73 mg, 0.6 mmol) in 4 mL dry DCM. The mixture is stirred for 24 h. at room temperature. After stirring, it was extracted with H_2O (2x10 mL) and DCM (2x20 mL). The residue was dried over Na_2SO_4, filtered and volatiles evaporated under vacuum. The crude product was purified by column chromatography with ethyl acetate:hexane (3:97) to yield an orange solid product. ^{1}H-NMR ($CDCl_3$, δ, ppm) = 8.13-8.11 (d, 4H), 7.88-7.86 (d, 8H), 7.47-7.45 (d, 6H), 4.32 (t, 4H), 1.79 (t, 4H), 1.51 (t, 4H) (Figure A.7).

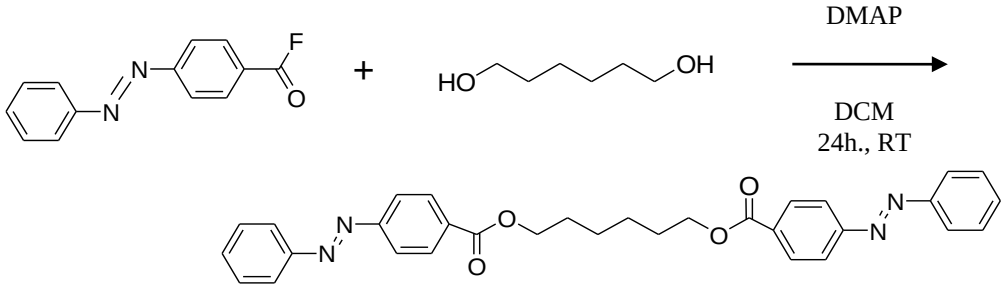

Figure 3.12. Synthesis of the linker AB-Hex-AB.

3.2.6. Synthesis of the linker 1,6-diadamantoyl- hexane (AD-Hex-AD)

3.2.6.1. Synthesis of Adamantane-1-carbonylfluoride. Adamantane-1-carbonylfluoride were synthesized according to a literature procedure [52] with slight modifications. A suspension of Adamantane-1-carboxylicacid (0.5 g, 2.7 mmol) and pyridine (0.437 mL, 5.4 mmol) in dry DCM (13.5 mL) was cooled to 0 °C under an argon atmosphere. To this was added cyanuric fluoride (0.464 mL, 5.4 mmol), and the contents were stirred for 90 min. A deep red/orange color was observed. Crushed ice/water (13.5 g) was then added, the suspension filtered, and the organic layer separated and washed with cold water (13.5 x 2 mL). Concentration in vacuo followed by chromatography (SiO2, 9:1 Hex/EtOAc) provided 0.353 g (64%) of Adamantane-1-carbonylfluoride as a white crystalline solid. ^{1}H NMR was as predicted in the agreement with the literature data.

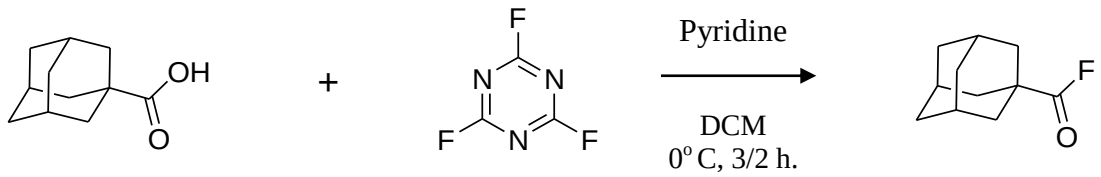

Figure 3.13. Synthesis of Adamantane-1-carbonylfluoride.

3.2.6.2. Synthesis of 1,6-diadamantoylhexane. The solution of Adamantane-1-carbonylfluoride (99 mg, 0.5 mmol) in 6 mL dry DCM was added to the suspension of Adamantoylhexanol (112 mg, 0.4 mmol) and DMAP (49 mg, 0.4 mmol) in 4 mL dry DCM. The mixture is stirred for 24 h. at room temperature. After stirring, it was extracted with H_2O (2x10 mL) and DCM (2x20 mL). The residue was dried over Na_2SO_4, filtered and volatiles evaporated under vacuum. The crude product was purified by column chromatography with ethyl acetate:hexane (0:100) to yield a white solid product. ^{1}H-NMR ($CDCl_3$, δ, ppm) = 4.02 (t, 4H), 1.99 (m, 6H), 1.86 (d, 12H), 1.69 (t, 12H), 1.61 (p, 4H), 1.36 (p, 4H) (Figure A.9).

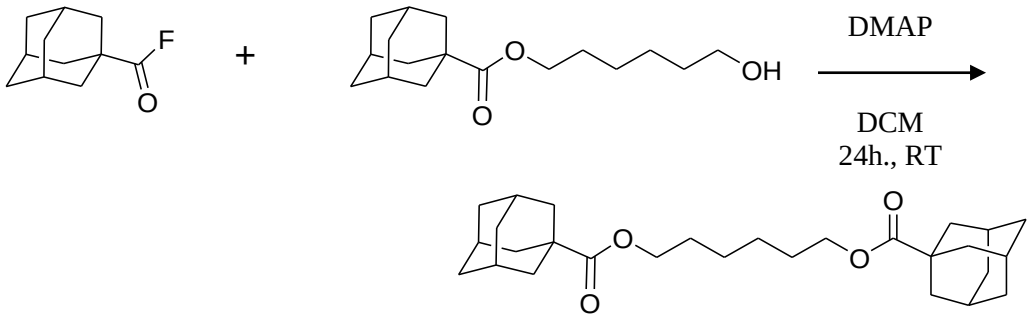

Figure 3.14. Synthesis of the linker AD-Hex-AD.

4. RESULTS AND DISCUSSIONS

4.1. Fabrication of Microcapsules

4.1.1. Functionalization of Au nanoparticles

Water soluble cyclodextrin (CD) functionalized gold nanoparticles have been used for making disordered supramolecular templates for more than a decade [54]. In this study literature examples were followed to obtain both β and α cyclodextrin coated AuNPs as described before (Figure 4.1). Average particle size was found to be about 6 nm.

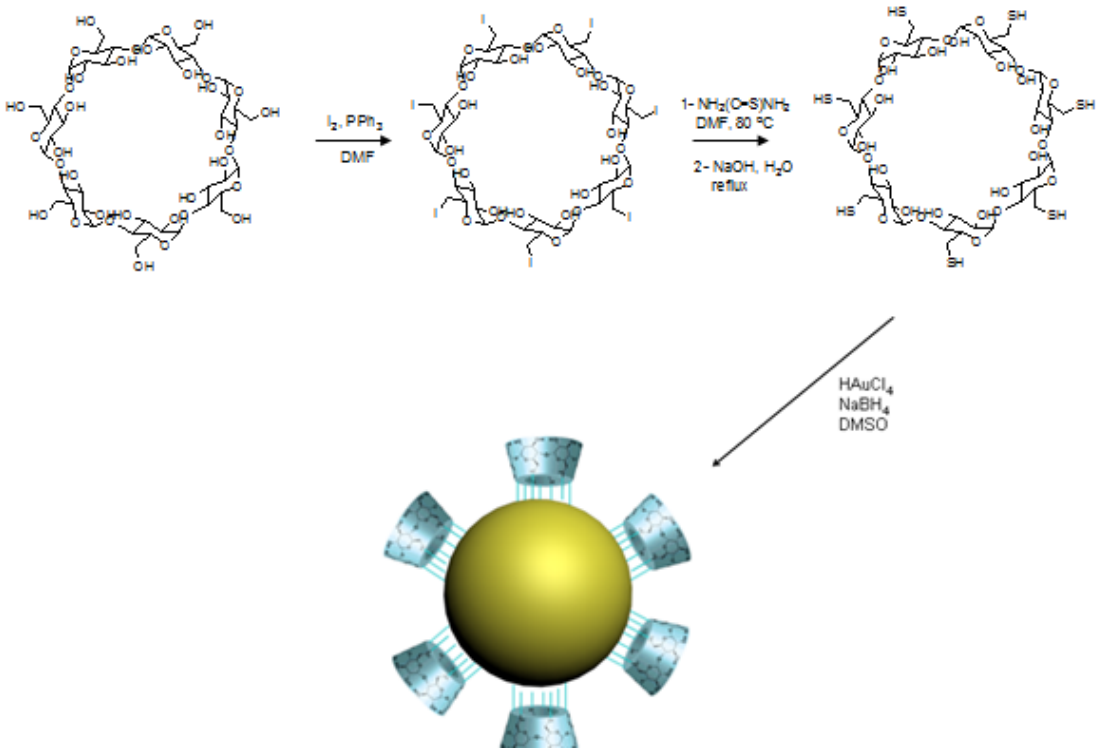

Figure 4.1. Synthesis steps of CD functionalized Au NPs.

4.1.2. Photoreversibility of crosslinker molecules

Azobenzenes are of well-known class of photo-responsive compounds that are able to reversibly isomerize from trans to cis form by irradiation at about 360 nm and from cis

to trans form by irradiation at 455 nm. Also it is well known that thermodinamically more stable trans-isomer form of azobenzene derivatives and α- cyclodextrins can form inclusion complexes via the specific host-guest interaction [22]. As well as fitting more into α-CDs, azobenzene can make inclusion complexes with β-CD to some extent.

In this study, four different crosslinkers were synthesized, three of them contain azobenzene moiety and one without azobenzene, to fabricate and investigate light-microcapsules. Each guest molecule is a homo/hetero-bifunctional noncovalent linker that carries has two identical or different supramolecular binding sites (Figure 4.2)

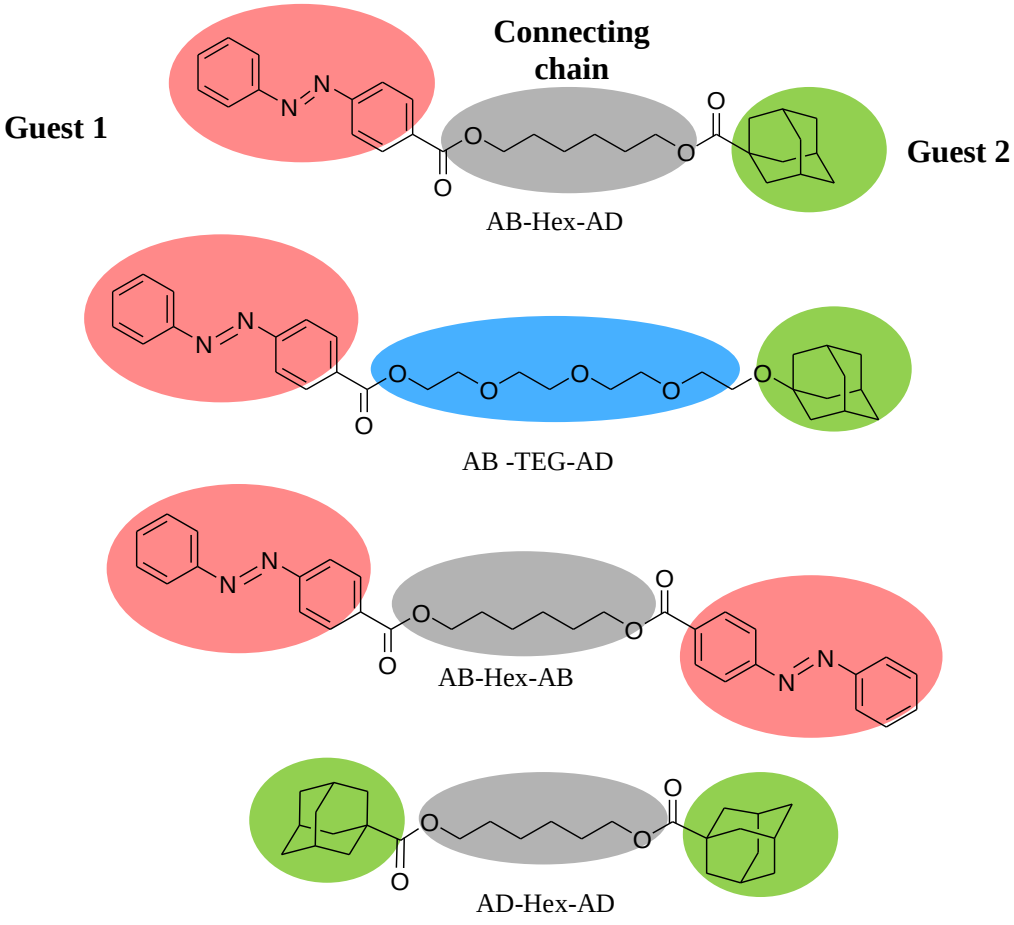

Figure 4.2. Structures of the crosslinkers used in this study.

As it is mentioned before, while azobenzene has a binding affinity towards α-CD, as well as β-CD weakly, adamantane unit is a suitable guest molecule for β-CD. Using these

difference, we could investigate the effects of different guest molecules and connecting chains on the photoreversible microcapsule systems.

4.1.3. Synthesis of Microcapsules

0.1 mL of linker solution in DCM was added into 2 mL of aqueous CD functionalized Au NP solution. The mixture was rapidly shaked. Since DCM is heavier than water DCM, microcapsules inside of which is full of DCM set at the bottom of the vial. After a few minute waiting, with the help of pipette microscapsules was removed carefully from the solution and added to another vial which is full of clean H_2O only (Figure 4.3). This cleaning process is repeated 2-3 times to remove the excess AuNP from the media. This microcapsule system was called dichloromethane-in-water system (Figure 4.4).

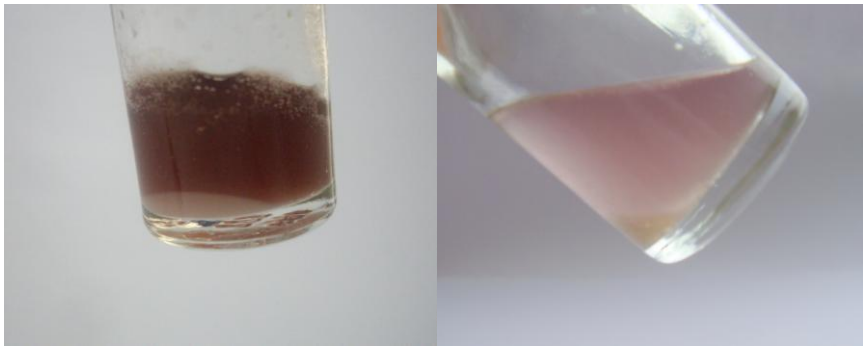

Figure 4.3. Microcapsules before and after cleaning of the media.

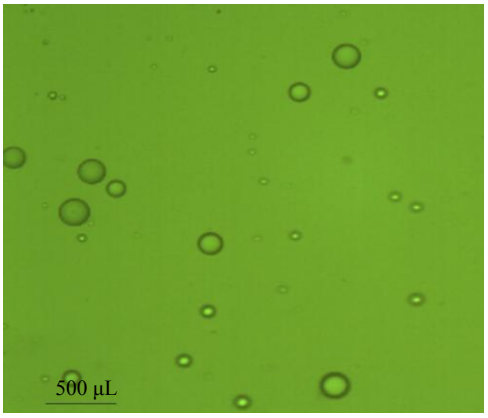

Figure 4.4. Microcapsules DCM in water.

To understand the behavour of crosslinker parts towards microcapsule formation, different microcapsule tests were done with different types of crosslinkers and nanoparticles.

4.1.4. Stability of Microcapsules

Reversible and weak nature of nanoparticles force them from order to disorder resulting in irreversible NP aggregation. To obtain controlled distribution of NPs and stable microcapsules not only the effect of the match between host and guest molecules but also other parameters such as solvent, consentration, hyrophilic property of bridging molecules should be taken into account.

Hydrophilicity is of great importance for the stabilizaton of microcapsules. For instance, while α-CD capped AuNPs form stable microcapsules with hydrophobic alkyl chain containing linker 1-adamantoyl-6-azobenzoylhexane (AB-Hex-AD), they don't form stable microcapsules with hydrophilic tetraethylene glycol (TEG) containing linker Adamantyl-(4-phenyl)azobenzoyl tetraethyleneglycol (AB-TEG-AD) (Figure 4.5). This formation difference between AB-TEG-AD and AB-Hex-AD used microcapsules proved the reason of deformation on AB-TEG-AD used microcapsules. This reason was the hydrophilic property of linker molecule.

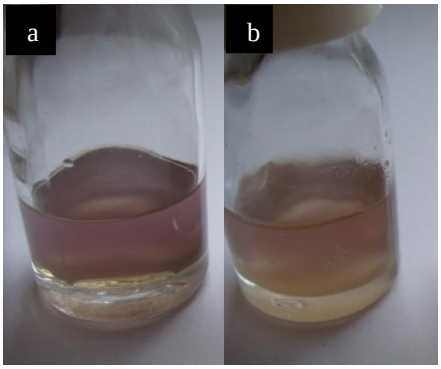

Figure 4.5. Microcapsule experiments of α-CD capped AuNPs with (a) AB-TEG-AD, and (b) AB-Hex-AD.

Trying different solvents showed us the selectivity of microcapsule formation depends on the solvent. While a microcapsule formation occurs between α -CD capped Au NP's and the linker 1-adamantoyl-6-azobenzoylhexane (AB-Hex-AD) with the use of chloroform and dichloromethane as the organic solvent, the formation does not occur with toluene. Otherwise microcapsule formation occurs between α-CD capped AuNPs and the linker 1,6- diazobenzoylhexane (AB-Hex-AB) using toluene as well as dichloromethane and chloroform as the organic solvent to some extent

Fabrication of microcapsules highly depend on the concentration of crosslinker and nanoparticle solution to control over the self-assembly. So that, microcapsules need spesific concentration of building blocks to get colloidal stabilization.

4.1.5. Microcapsule Fabrication with α-CD coated AuNPs

Microcapsules with different crosslinkers were prepared with the same strategy previously mentioned in the section 4.1.3 (Synthesis of Microcapsules). Microcapsules between linkers and α -CD capped Au NP's were synthesized with the use of $CHCl_3$ and DCM as the organic phase solvents. Lots of different concentration were tried to form microcapsules and the most stable concentration for the each microcapsule was chosen.

4.1.5.1. Microcapsules with α-CD AuNPs and Adamantyl-(4-phenyl)azobenzoyl tetraethyleneglycol (AB-TEG-AD). Azobenzene (AB) as a guest molecule fits into α-CD host, while the size of adamantane (AD) is suitable for larger sized host molecule β-CD. Though, some kind of unstable microcapsule formation was observed between α-CD functionalized AuNP and crosslinker with AD and AB on it. Herein, very less stability of microcapsules was observed despite being used their most stable concentration that they remained only a few hours like 2-3 hours after cleaning process. Then the capsules began to aggregate (Figure 4.5a). These microcapsules were the largest and the most unstable ones among the microcapsules formed with α-CD AuNPs (Figure 4.6a). The unstability of them could be the reason of hydrophilic property of the connecting chain tetraetyhlene glycol (TEG).

4.1.5.2. Microcapsules with α-CD coated AuNPs and 1-Adamantoyl-6-(4-phenylazo)benzoyl-Hexane (AB-Hex-AD). Microcapsules prepared with α-CD AuNPs and AB-Hex-AD were more stable and smaller than with α-CD AuNPs and AB-TEG-AD ones (Figure 4.6b). Although being not stable enough for microcapsules, they remained 1-2 days longer than the remaining time of AB-TEG-AD used microcapsules. This stability proved the impact of the hydrophilicity of crosslinker on microcapsule fabrication (Figure 4.5b).

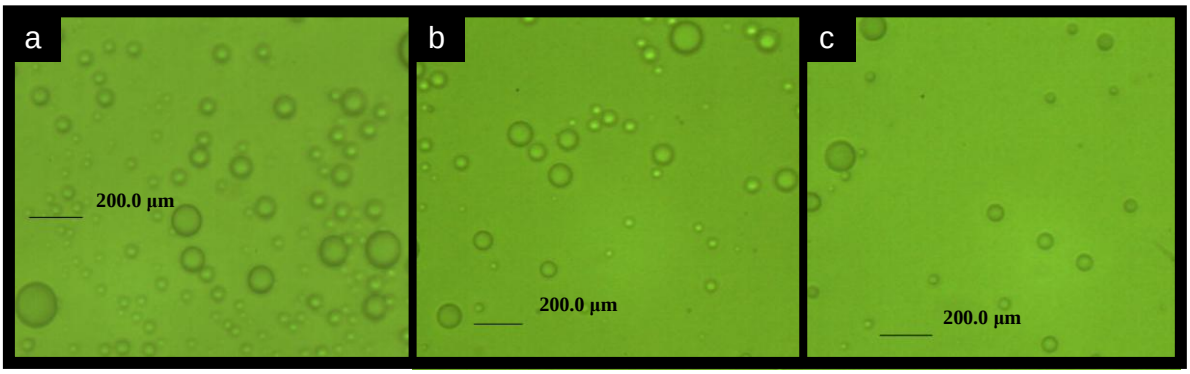

Figure 4.6. Microcapsules formed by α-CD NPs with (a) AB-TEG-AD, (b) AB-Hex-AD, and (c) AB-Hex-AB.

4.1.5.3. Microcapsules with α-CD coated AuNPs and 1,6-di(4-(phenyldiazenyl)benzoyl)-hexane (AB-Hex-AB). Due to the perfect match between AB and α-CD, two sided azobenzene containing crosslinker provided strong bridge between nanoparticles and formed stable microcapsules. These were the most stable and the smallest microcapsules among all α-CD AuNPs used microcapsules (Figure 4.6c). They remained more than 1 week.

4.1.5.4. Microcapsules with α-CD coated AuNPs and 1,6-diadamantoyl-hexane (AD-Hex-AD). As a control experiment microcapsule fabrication between α-CD AuNPs and two sided adamantane containing AD-Hex-AD crosslinker were tried. Because microcapsules fabrication between one sided adamantane containing crosslinkers (AB-Hex-AD and AB-TEG-AD) were achieved although they were unstable. This time microcapsule formation didn't occur. It was reasonable because adamantane is bigger than the inner cavity of α-CD. There couldn't be suitable interaction between adamantane and α-CD. So it was

understood that the forces in the formation of microcapsules between AB-Hex-AD and/or AB-TEG-AD and α-CD AuNPs were more than host-guest interaction.

4.1.6. Microcapsule Fabrication with β-CD coated AuNPs

Microcapsules with different crosslinkers and organic solvents ($CHCl_3$ and DCM) were prepared with the same strategy previously mentioned in the section 4.1.3 (Synthesis of Microcapsules).

4.1.6.1. Microcapsules with β-CD AuNPs and Adamantyl-(4-phenyl)azobenzoyl tetraethyleneglycol (AB-TEG-AD). As expected, microcapsule fabrication between β-CD AuNPs and AB-TEG-AD resulted in unstable large microcapsules (Figure 4.8a). Despite the fact that azobenzene has a binding towards β-CD to some extent, it is not a strong binding. Also there is another parameter preventing the microcapsule formation which is the hydrophilicty of TEG molecule. Because of these reasons microcapsules were such unstable that they remained only a few minutes like 2-3 minutes after cleaning process. Then, they began to aggregate (Figure 4.7).

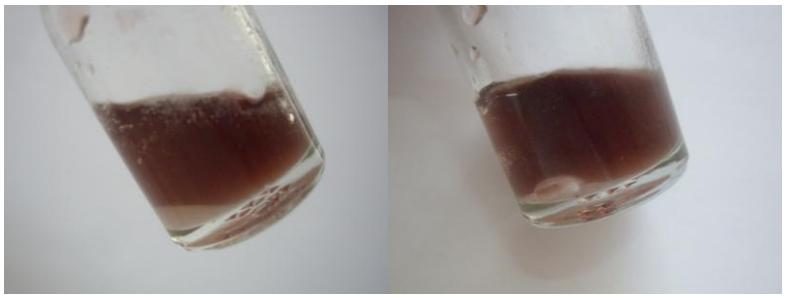

Figure 4.7. Before and after aggregation of microcapsules.

4.1.6.2. Microcapsules with β-CD coated AuNPs and 1-Adamantoyl-6-(4-phenylazo)benzoyl-Hexane (AB-Hex-AD). Microcapsules formed by using β-CD AuNPs and AB-Hex-AD were more stable and smaller than with β-CD AuNPs and AB-TEG-AD ones. But, they were too large and unstable in proportion to stable microcapsules (Figure 4.8b). They remained nearly one day.

4.1.6.3. Microcapsules with β-CD coated AuNPs and 1,6-di(4-(phenyldiazenyl)benzoyl)-hexane (AB-Hex-AB). Since interaction of azobenzene with β-CD is a weak noncovalent interaction, β-CD AuNPs and AB-Hex-AB formed unstable and large microcapsules (Figure 4.8c). Lifetime of the microcapsules was around 5 hours which is less than the remaining time of MCs with AB-Hex-AD and β-CD AuNPs. In this case unstability may be the reason of the absence of adamantane an appropriate binding unit towards β-CD.

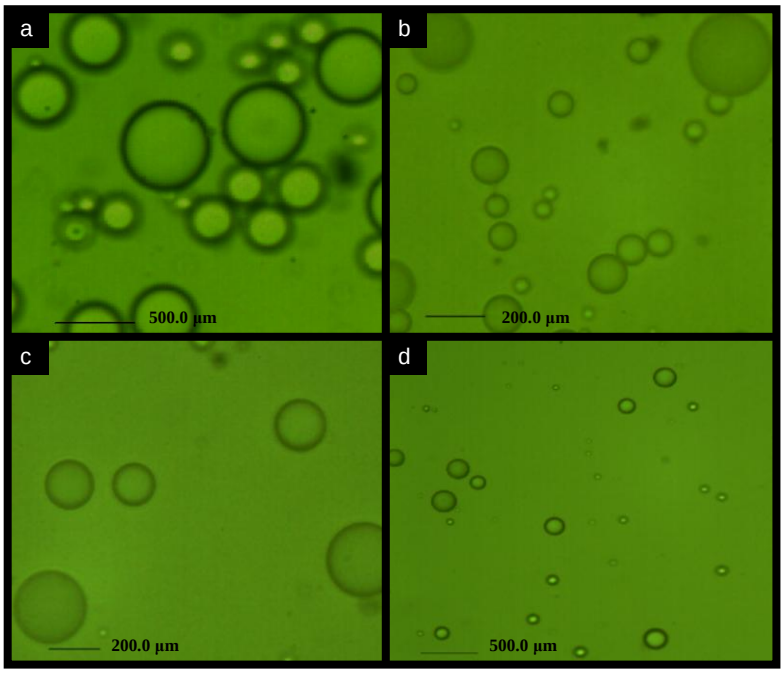

Figure 4.8. Microcapsules formed by β-CD NPs with (a) AB-TEG-AD, (b) AB-Hex-AD, (c) AB-Hex-AB, and (d) AD-Hex-AD.

4.1.6.4. Microcapsules with β-CD coated AuNPs and 1,6-diadamantoyl-hexane (AD-Hex-AD). Two sided AD containing crosslinker performed strong bridging interaction with β-CD coated nanoparticles and formed stable microcapsules on account of the perfect match between adamantane and β-CD units. These were the most stable and the smallest microcapsules among all β-CD AuNPs used microcapsules (Figure 4.8d). They remained more than one week.

4.1.7. Comparison for stabilization of synthesized microcapsules

Different microcapsule experiments were performed with different nanoparticles and crosslinkers. These experiments gave us some important informations about behavior of the building blocks.

While AB is a suitable guest for α-CD, AD is the best candidate for β-CD. Accordingly, the most stable microcapsules were the ones between these hosts and their appropriate homobifunctional guest molecule. It means that microcapsules formed by AB-Hex-AB with α-CD AuNPs and microcapsules formed by AD-Hex-AD with β-CD AuNPs were the most stable microcapsules with their strong noncovalent interaction.

On the other hand, each nanoparticle showed microcapsule formation more or less. Since interaction of azobenzene with β-CD is a weak noncovalent interaction, β-CD AuNPs formed unstable and large microcapsules with AB-Hex-AB/AB-Hex-AD/AB-TEG-AD. Furthermore, though α-CD does not interact with adamantane unit, α-CD AuNPs formed unstable and large microcapsules. Some of them has longer remaining time in proportion to others. The unstability of microcapsules formed by TEG based crosslinker is because of the hydrophilic property of the connecting chain tetraetyhlene glycol (TEG).

4.1.8. Transmission Electron Microscopy

Transmission Electron Microscope is a kind of microscope which uses electrons as source instead of ‘light’ as in a light microscope. TEMs are able to image at significantly higher resolution than light microscope. For instance one can see an object of a few angstrom (10^{-10} m) with fine details.

Since it is proved that the best interaction between nanoparticles and crosslinkers used in this project was the one with α-CD AuNPs and AB-Hex-AB. For the characterization of these stable microcapsules the project focused on, TEM images of the MCs were taken at different scales and proved the microcapsule formation as well as the aggregation of nanoparticles (Figure 4.9).

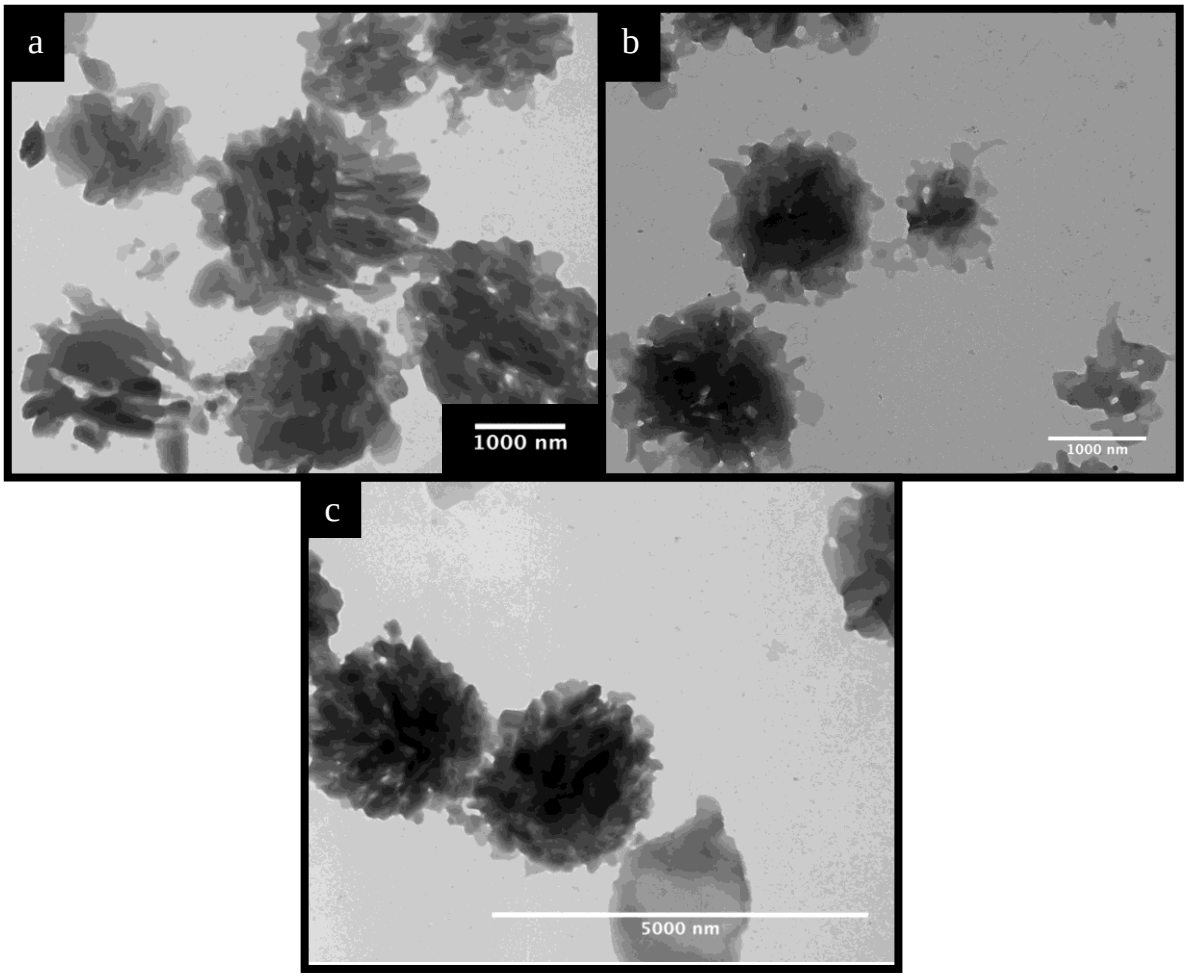

Figure 4.9. TEM images of microcapsules at different scales.
The scales are 1000 nm, (a), (b), and 5000 nm (c).

4.2. Photoreversibility of Microcapsules

Photoreversibility is one of the important characteristics of self-assembled microcapsules in this project. In order to investigate the effect of photoreversibility on microcapsules time-dependent UV-absorbance peak shifts of crosslinkers were checked.

4.2.1. Time-dependent UV Absorption of Crosslinkers

Each azobenzene containing crosslinker was irradiated at 365 nm. As expected, UV absorbance peak shift was detected by time due to the photoisomerization of azobenzene (Figure 4.10).

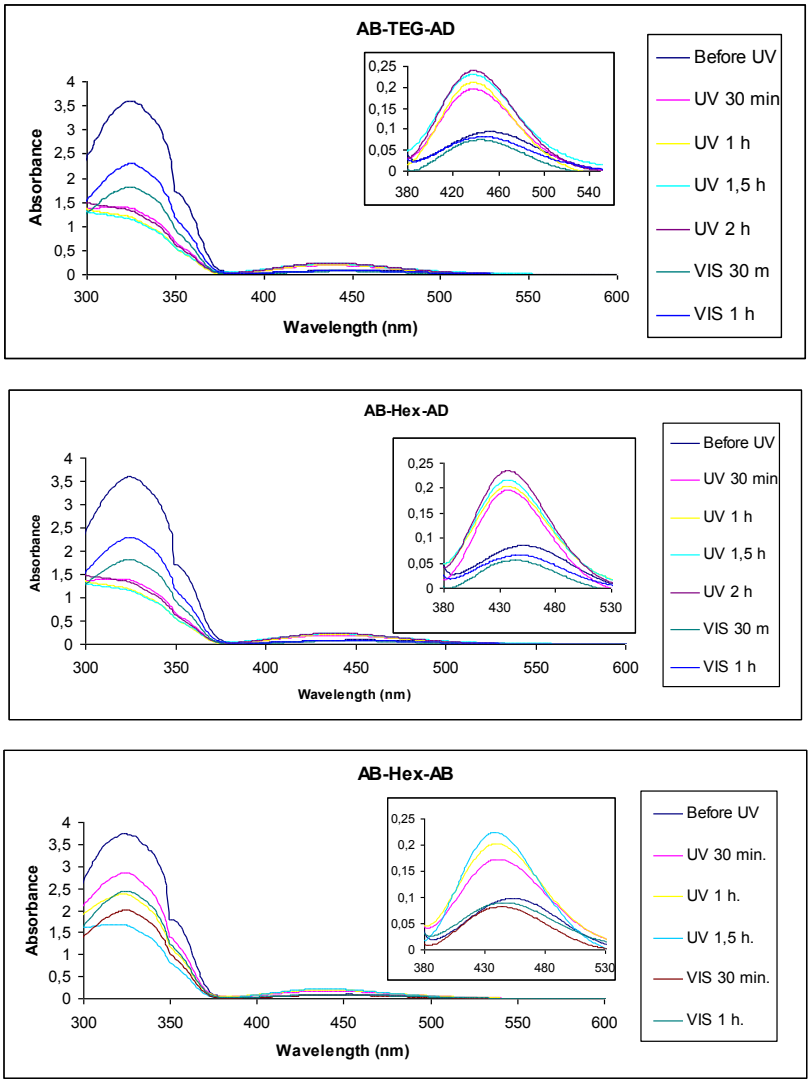

Figure 4.10. UV-Vis spectra of photoswitchable crosslinkers.

At 365 nm the absoption band at around 323 nm highly decreased, and the band at around 450 nm increased slightly. Because it is a reversible process, when irradiated by visible light, at 450 nm the absorption increased again, which proved the photoisomerization property of azobenzene containing crosslinkers.

4.2.2. Future Studies

Studies are in progress for photoreversibility of microcapsules.

5. CONCLUSIONS

A new strategy for the construction of stable microcapsules via supramolecular self-assembly was developed. Microcapsules were prepared by noncovalent crosslinking of different types of water soluble cyclodextrin coated gold nanoparticles and organo-soluble homo/heterobifunctional crosslinker molecules via the specific host-guest interaction. We have also developed a photoreversible supramolecular system by using light- crosslinker as one of the building blocks in microcapsules. As the building blocks of microcapsules, different types of nanoparticles (α-CD AuNPs, β-CD AuNPs) and azobenzene and/or adamantane functionalized crosslinker molecules (AB-TEG-AD, AB-Hex-AD, AB-Hex-AB, and AD-Hex-AD) were used.

According to specific host-guest complexation between α-CD and azobenzene, and β-CD and adamantane, the most stable microcapsules were the ones between these hosts and their appropriate homobifunctional guest molecules. As a result, the microcapsules formed by AB-Hex-AB with α-CD AuNPs and formed by AD-Hex-AD with β-CD AuNPs were the most stable microcapsules with their strong noncovalent interaction.

On the other hand, each nanoparticle showed microcapsule formation more or less. Since interaction of azobenzene with β-CD is a weak noncovalent interaction, β-CD AuNPs formed unstable and large microcapsules with AB-Hex-AB/ AB-Hex-AD/ AB-TEG-AD. Furthermore, though α-CD does not interact with adamantane unit, α-CD AuNPs formed unstable and large microcapsules adamantane containing AB-Hex-AD/ AB-TEG-AD crosslinkers.

The photoreversible nature of the azobenzene containing crosslinker molecules were proved by UV-Vis Absorption Spectroscopy. However, the photoreversibility of microcapsules is a topic still in progress.

APPENDIX A: SPECTROSCOPY DATA

^{1}H NMR and IR spectroscopy data of the newly synthesized products are included.

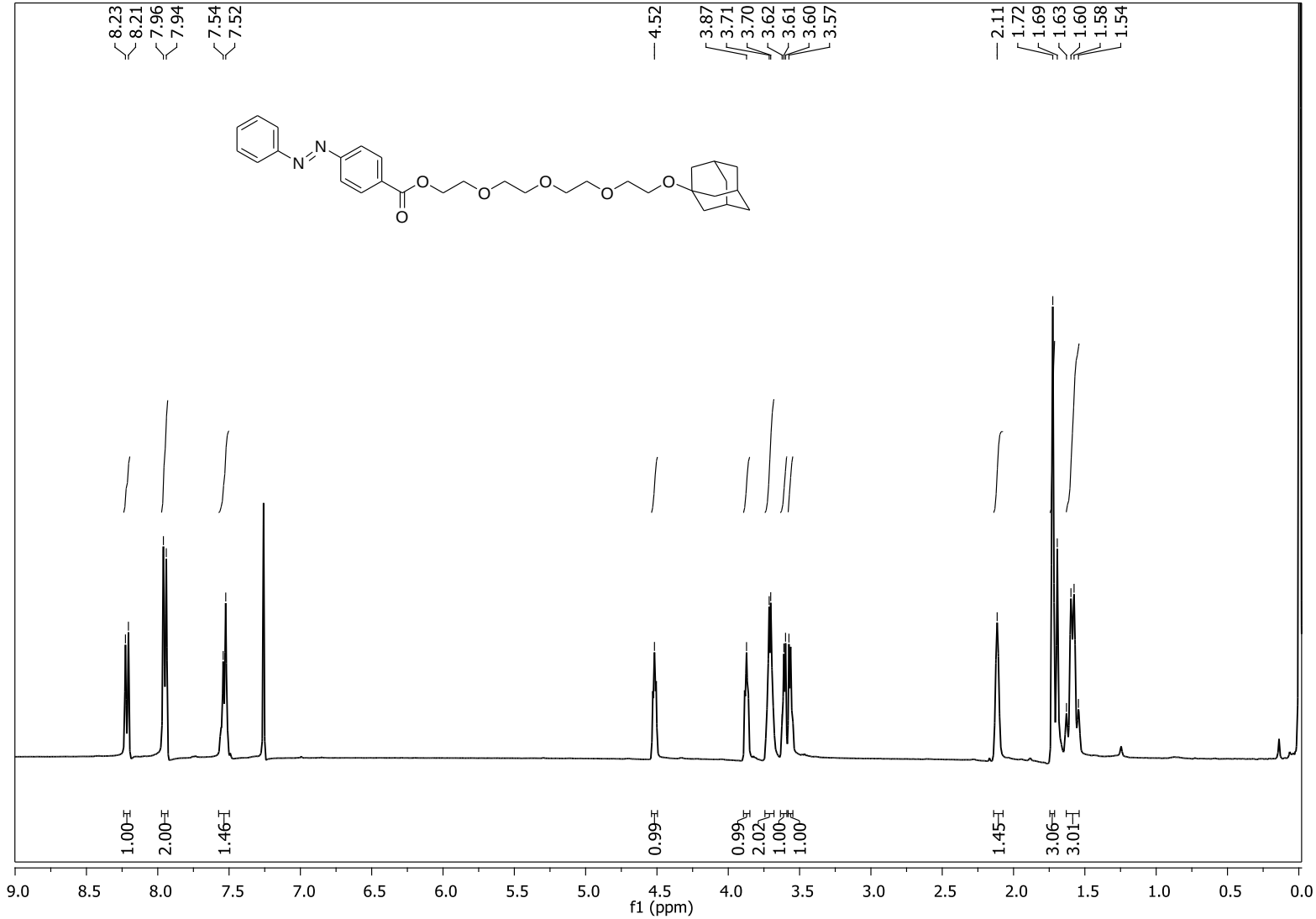

Figure A.1. ^{1}H-NMR of the linker AB-TEG-AD.

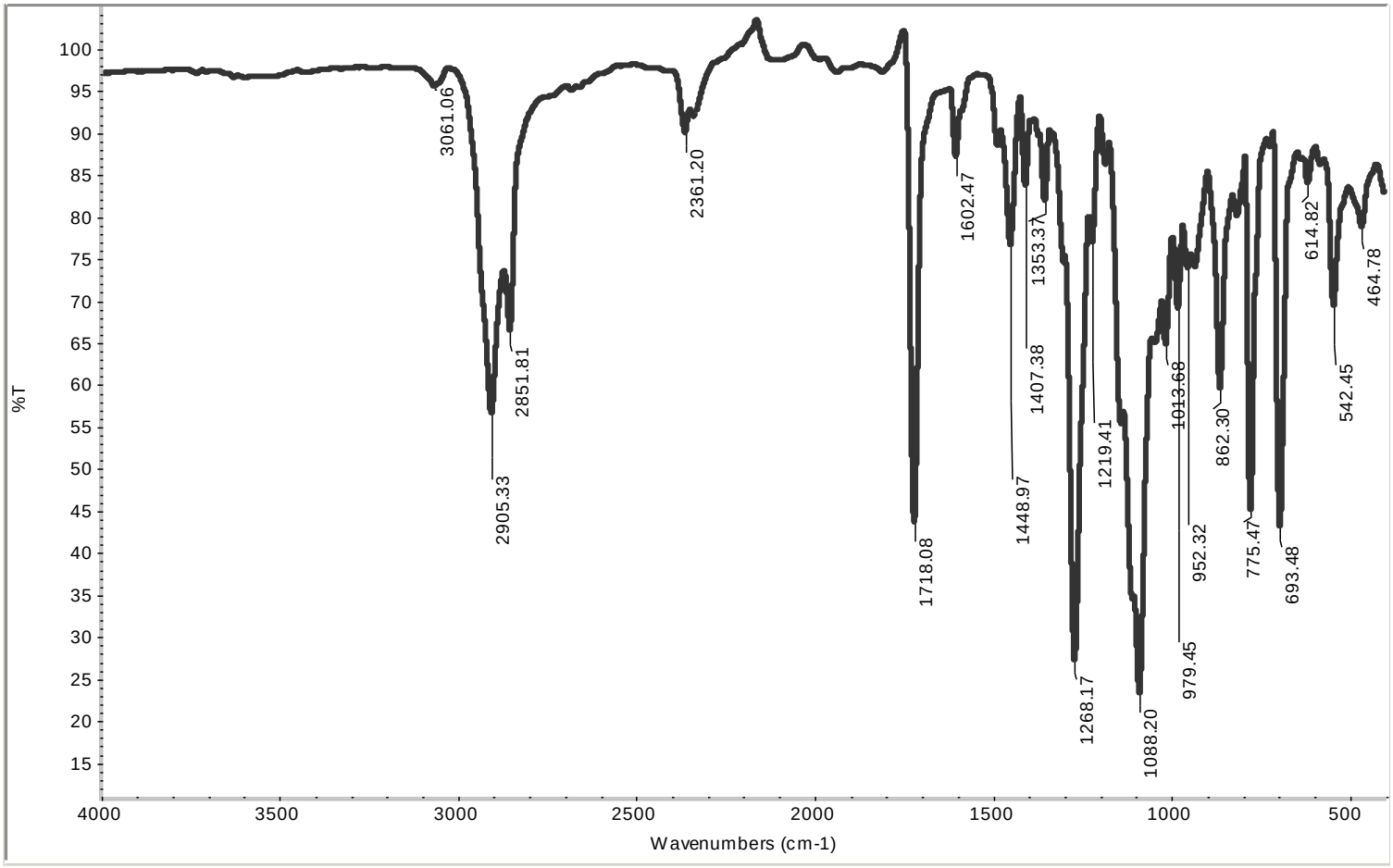

Figure A.2. IR of the linker AB-TEG-AD.

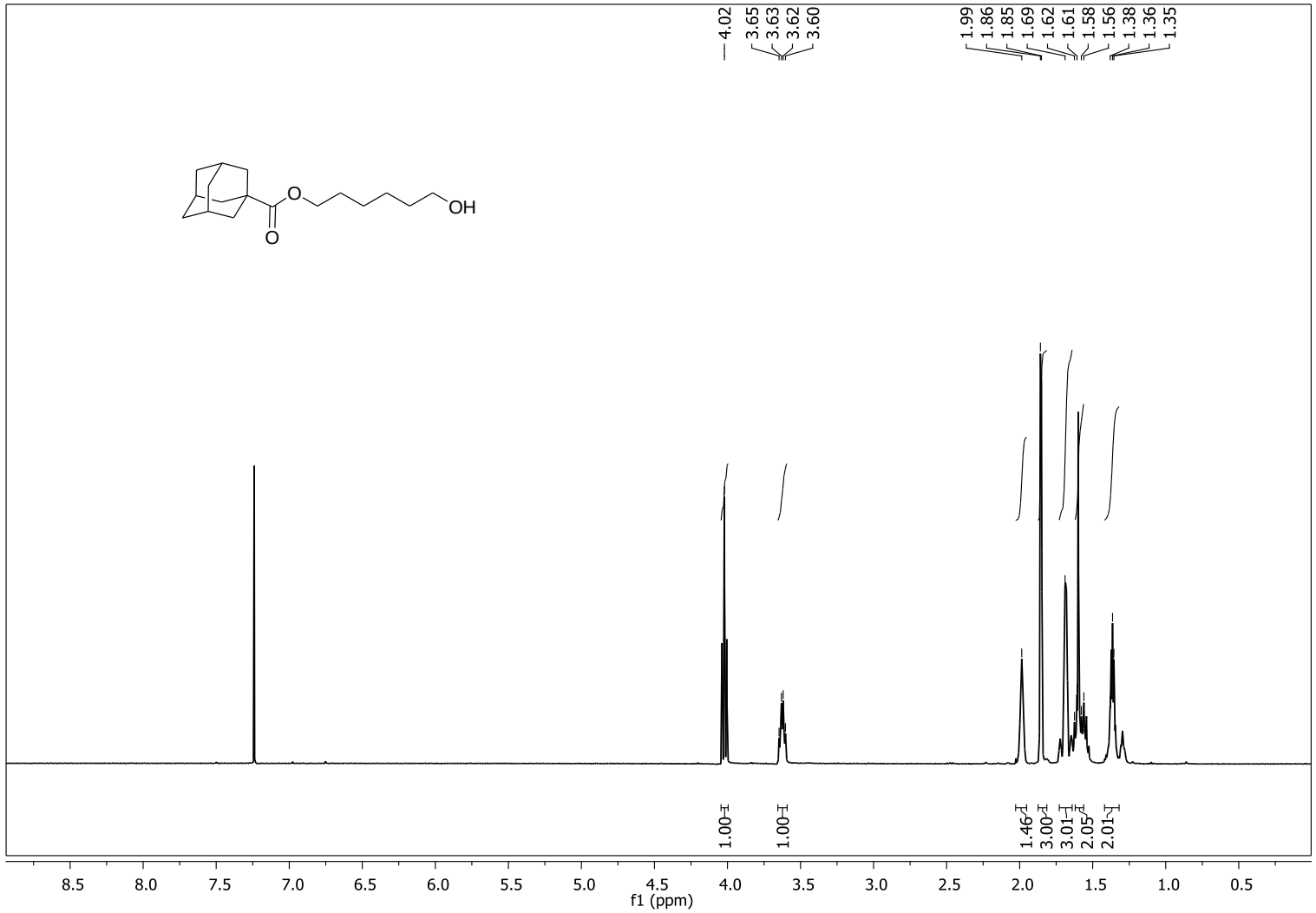

Figure A.3. ^{1}H-NMR of the molecule AD-Hex-ol.

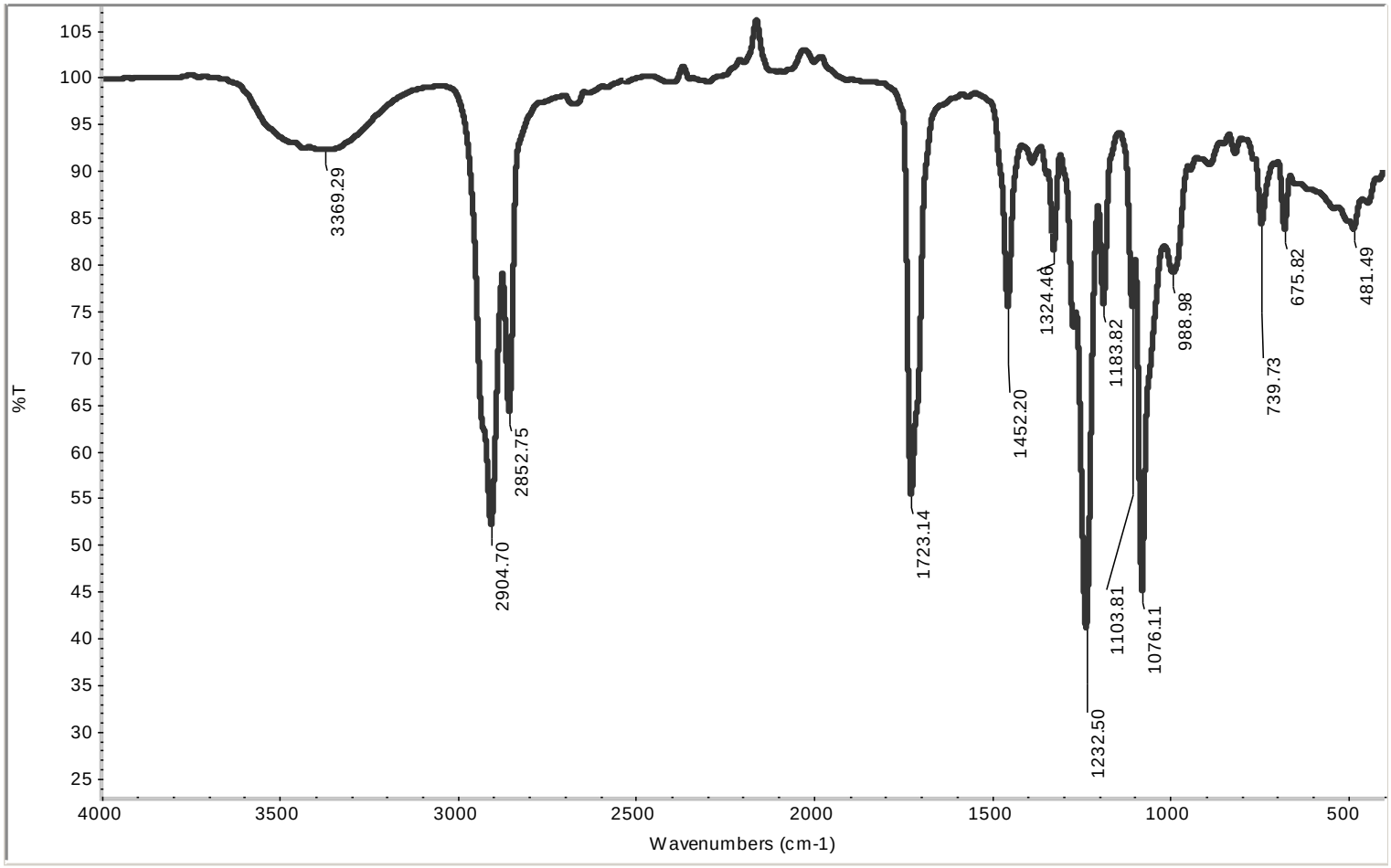

Figure A.4. IR of the molecule AD-Hex-ol.

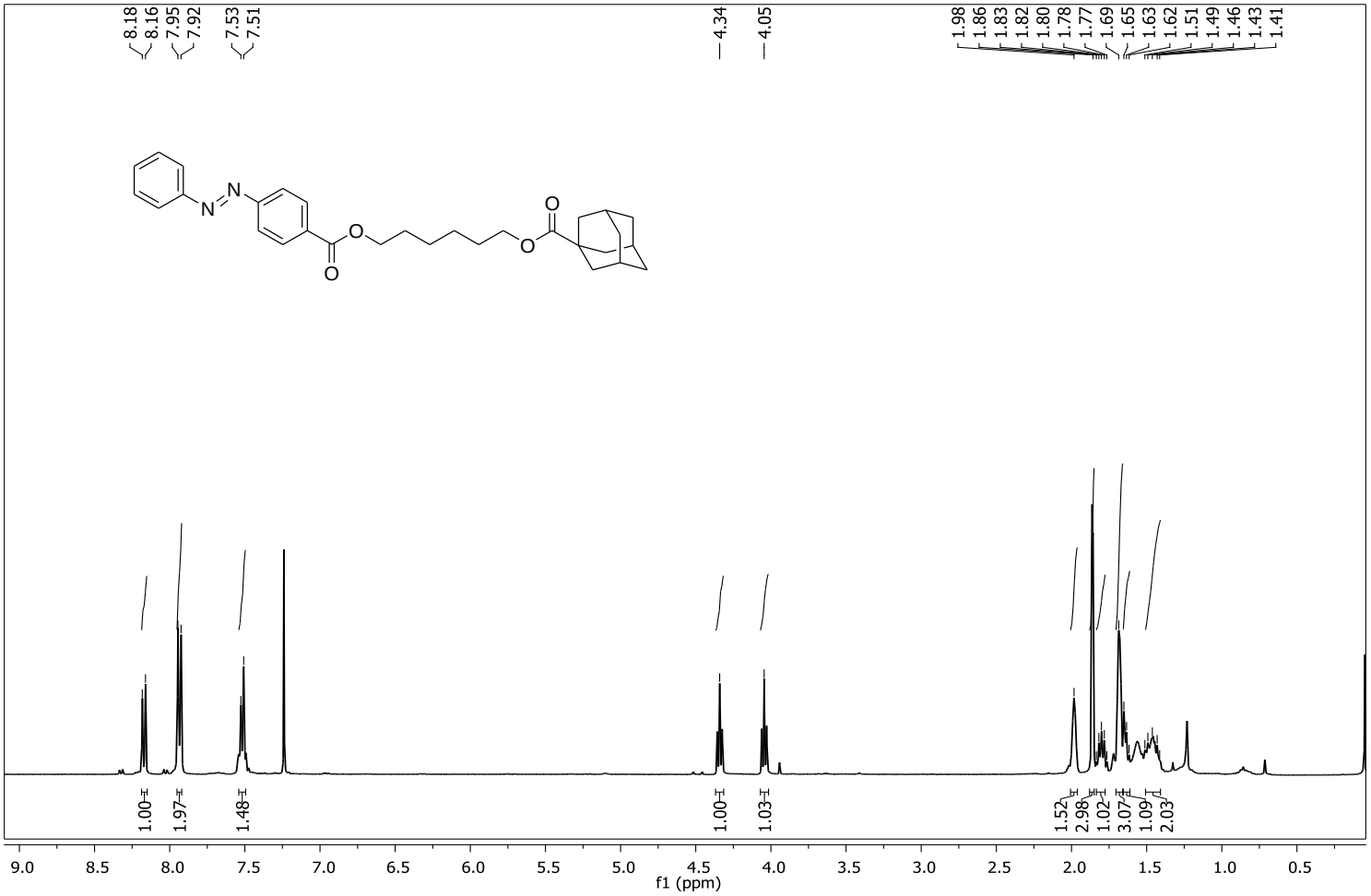

Figure A. 5. ^{1}H-NMR of the linker AB-Hex-AD.

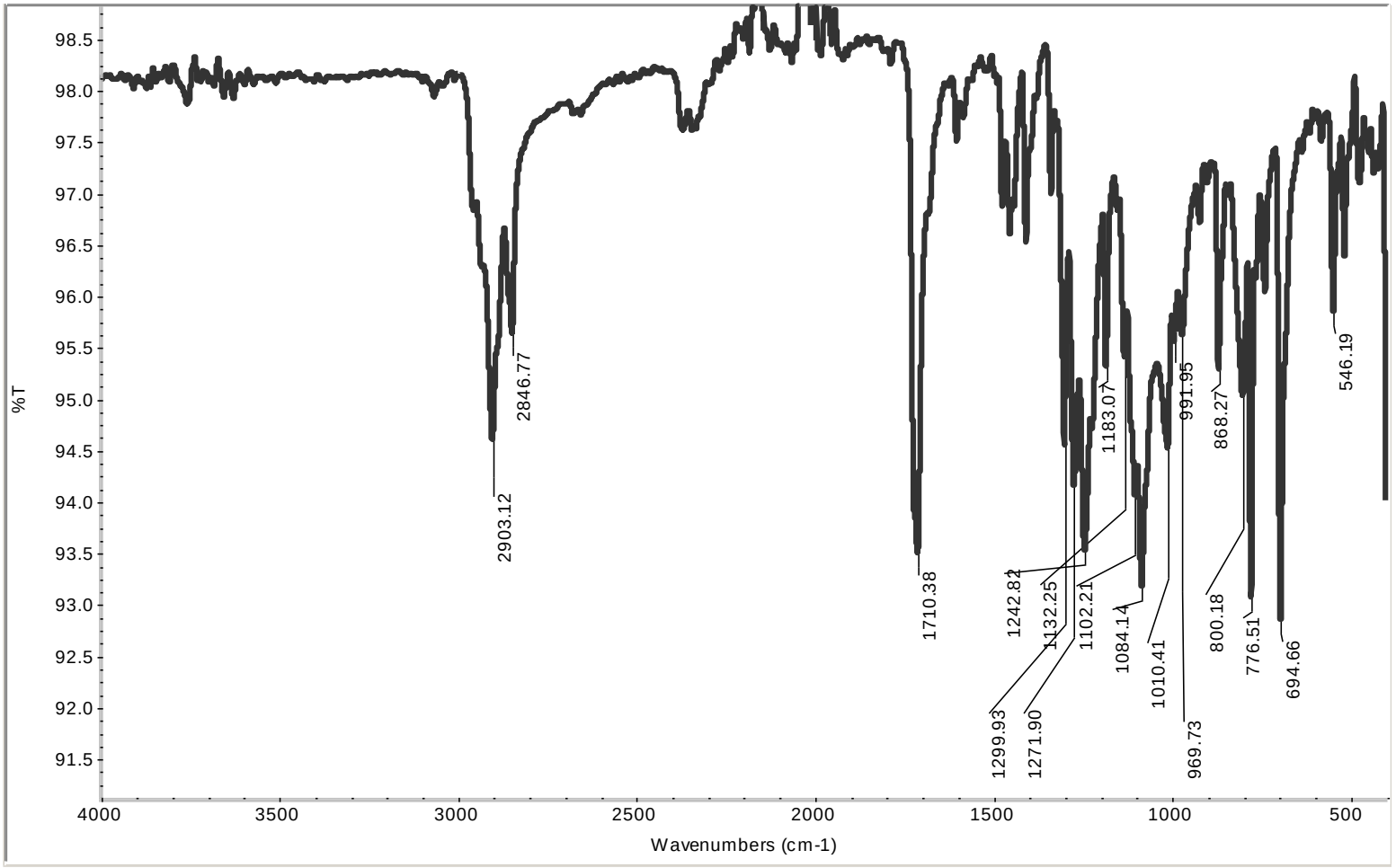

Figure A.6. IR of the linker AB-Hex-AD.

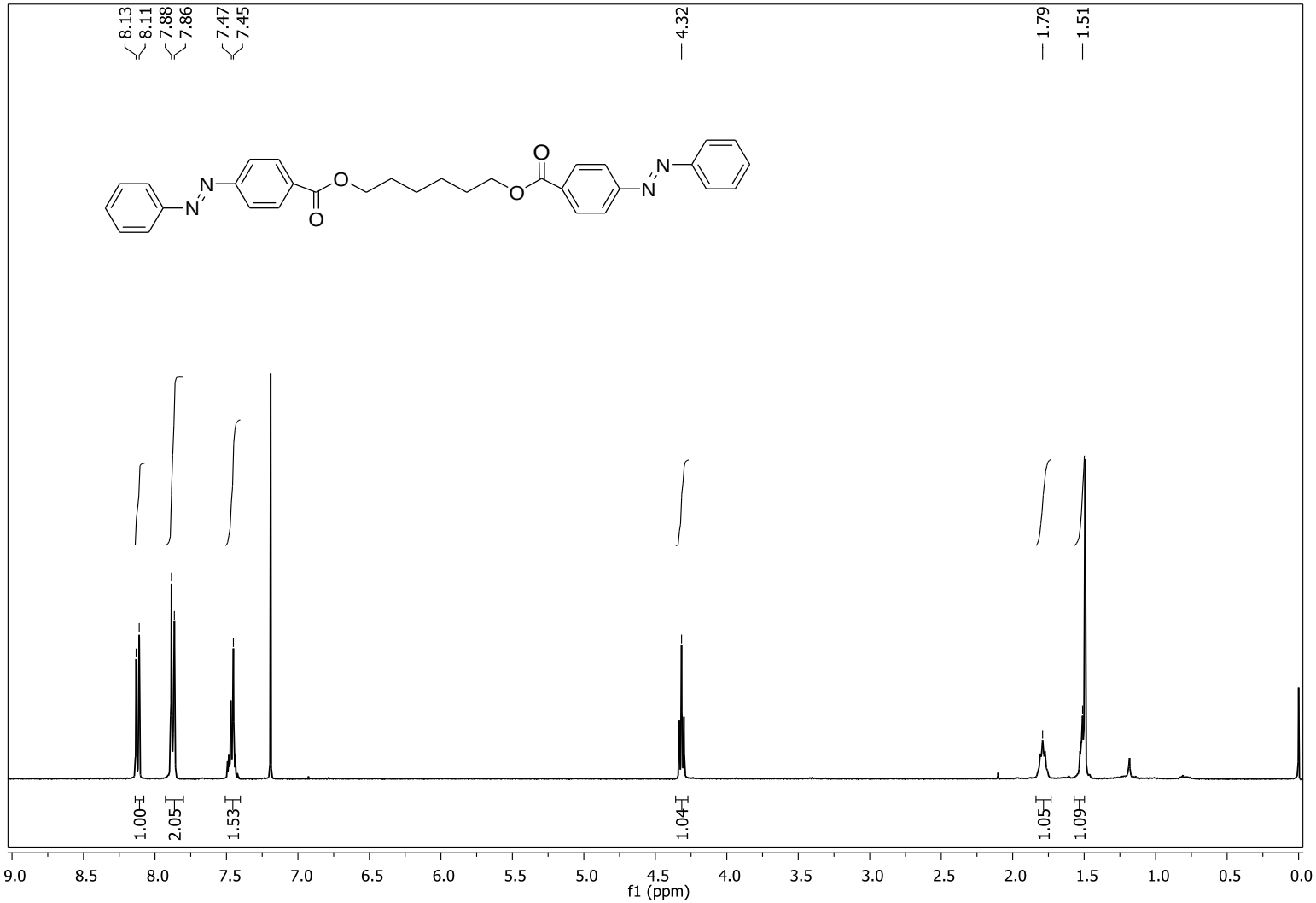

Figure A.7. ^{1}H-NMR of the linker AB-Hex-AB.

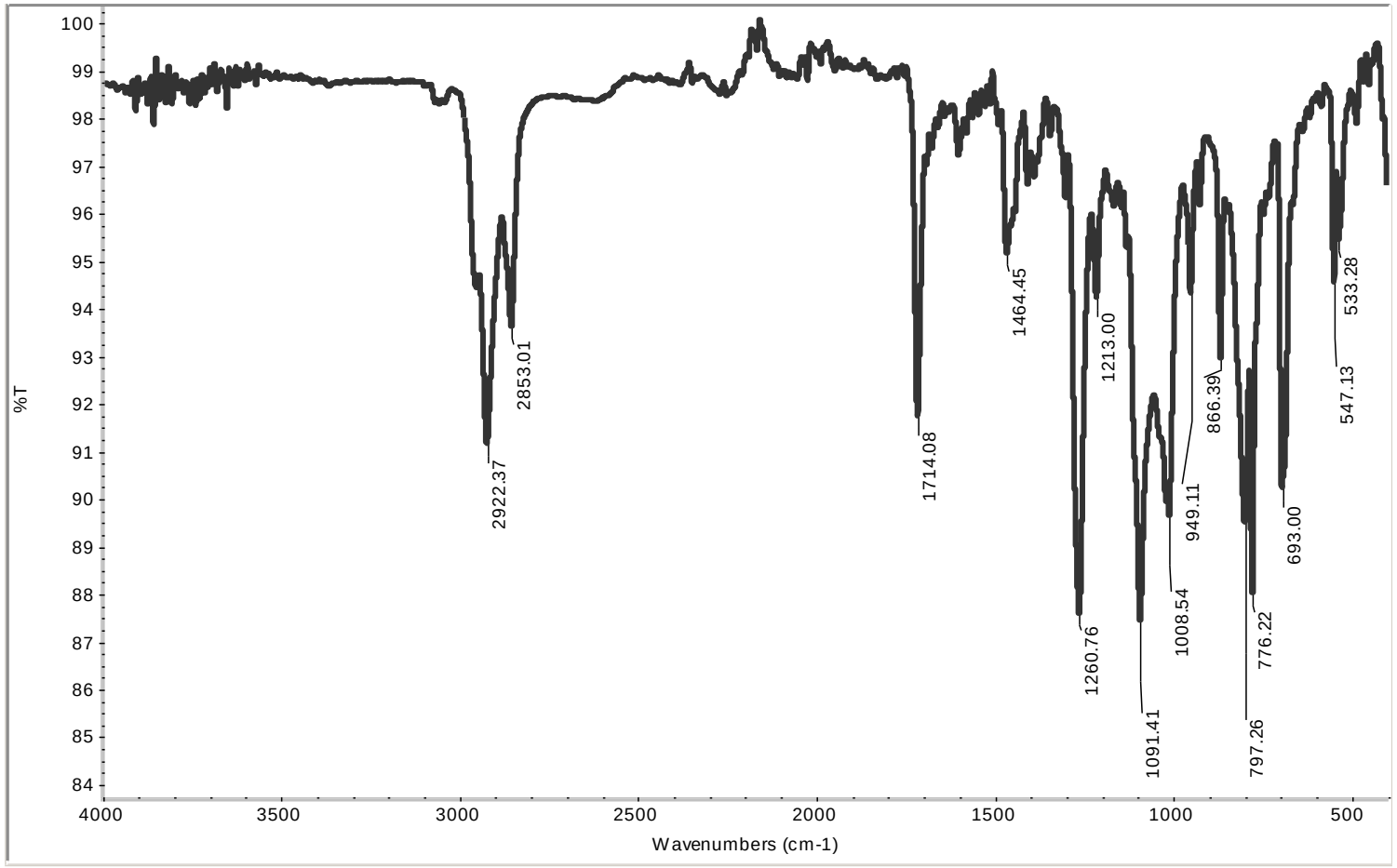

Figure A.8. IR of the linker AB-Hex-AB.

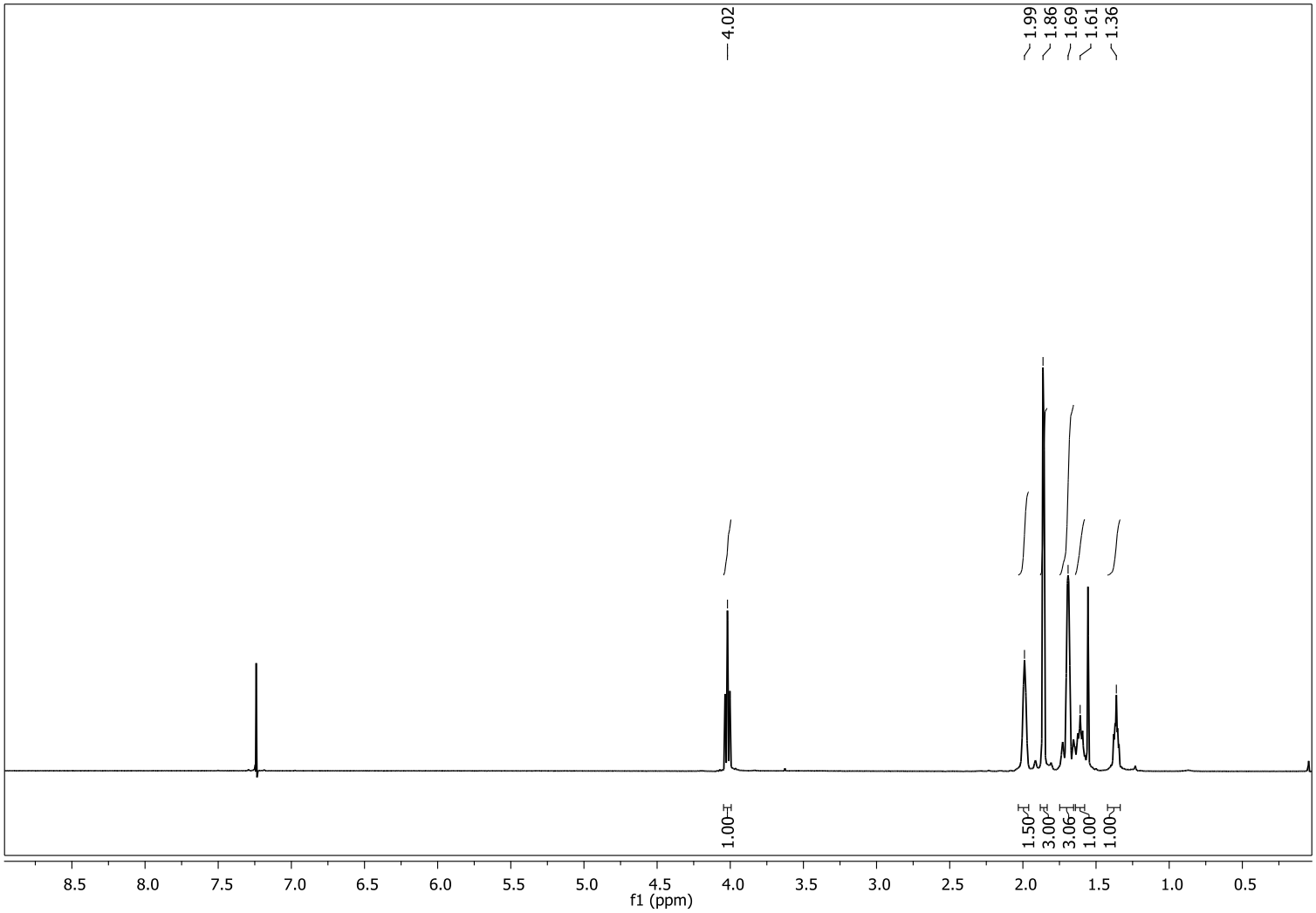

Figure A.9. ^{1}H-NMR of the linker AD-Hex-AD.

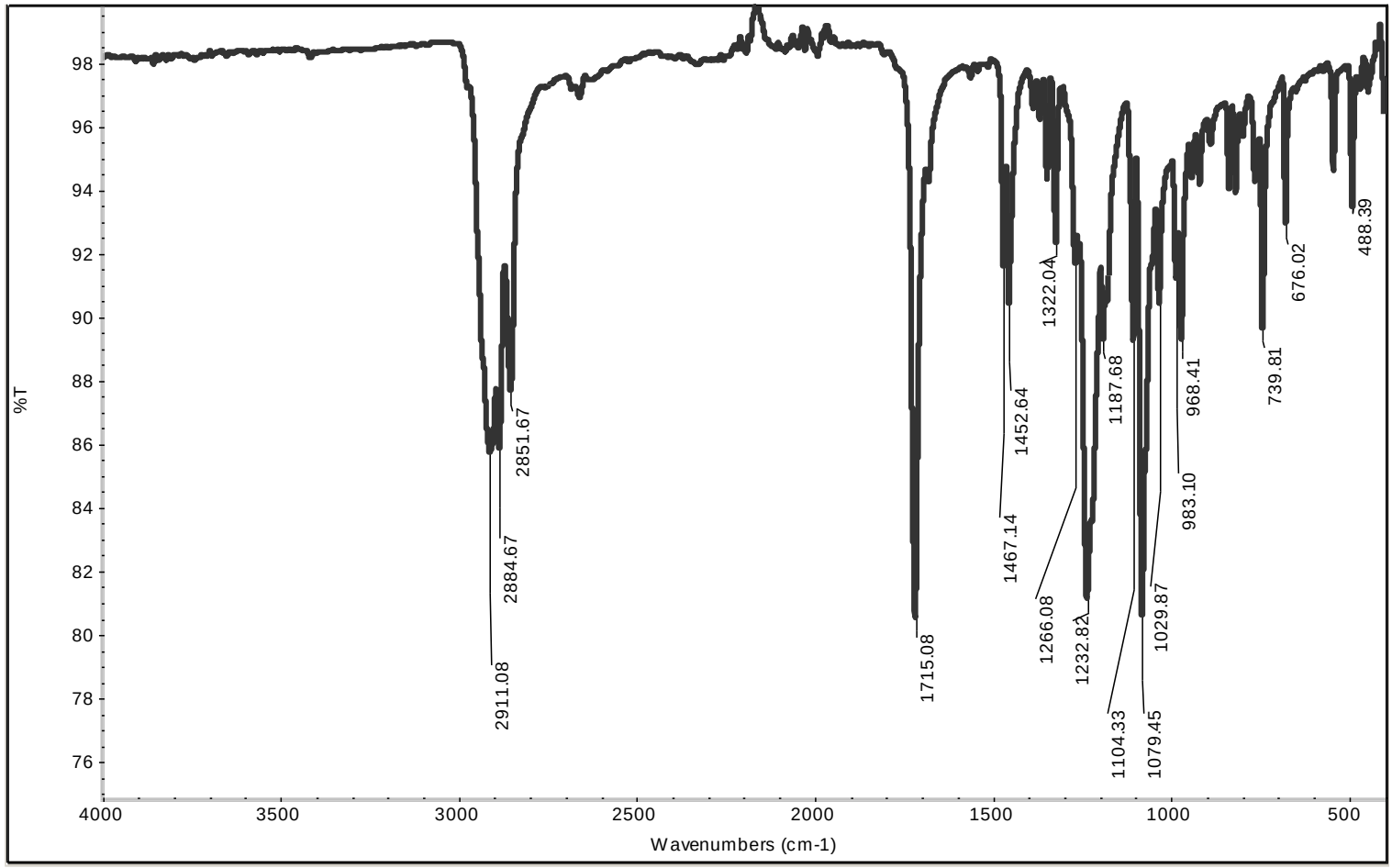

Figure A.10. IR of the linker AD-Hex-AD.

REFERENCES

1. Alberts, B., A. Johnson, J. Lewis, M. Raff, K. Roberts and P. Walter, *Molecular Biology of the Cell*, Garland Science, New York, NY, USA, 2002.

2. Rothemund, P. W. K., "Folding DNA to create nanoscaleshapes and patterns", *Nature*, Vol. 440, pp. 297-302, 2006.

3. Woodhead, J. L. and C. K. Hall, "Encapsulation Efficiency and Micellar Structure of Solute-Carrying Block Copolymer Nanoparticles", *Macromolecules*, Vol. 44, No. 13, pp. 5443-5451, 2011.

4. Kim, Y. J., S. Y. Chai and W. I. Lee, "Control of TiO_2 Structures from Robust Hollow Microspheres to Highly Dispersible Nanoparticles in a Tetrabutylammonium Hydroxide Solution", *Langmuir*, Vol. 23, No. 19, pp. 9567-9571, 2007.

5. Wang, K., D. S. Guo, X. Wang and Y. Liu, "Multistimuli Supramolecular Vesicles Based on the Recognition of p-Sulfonatocalixarene and its Controllable Release of Doxorubicin", *ACS Nano*, Vol. 5., No. 4, pp. 2880-2894, 2011.

6. Sanyal, A., B. T. Norsten, O. Uzun and V. M. Rotello, "Adsorption/Desorption of Mono- and Diblock Copolymers on Surfaces Using Specific Hydrogen Bonding Interactions", *Langmuir*, Vol. 20, No. 14, pp. 5958-5964, 2004.

7. Patra, D., F. Ozdemir, O. R. Miranda, B. Samanta, A. Sanyal and V. M. Rotello, "Formation and Size Tuning of Colloidal Microcapsules via Host−Guest Molecular Recognition at the Liquid−Liquid Interface", *Langmuir*, Vol. 25, No. 24, pp. 13852-13854, 2009.

8. Whitesides, G. M. and B. Grzybowski, "Self-Assembly at all Scales", *Science*, Vol. 295, No. 5564, pp. 2418-2421, 2002.

9. Steed, J. W. and J. L. Atwood, *Supramolecular Chemistry*, John Wiley & Sons, New York, 2000.

10. Nguyen, S. B. T., D. L. Gin, J. T. Hupp and X. Zhang, "Supramolecular Chemistry: Functional structures on the mesoscale", *PNAS*, Vol. 98, No. 21, pp. 11849–11850, 2001.

11. Stella, V. J. and R. A. Rajewski, "Cyclodextrins: Their future in drug formulation and delivery", *Pharmaceutical Research*, Vol. 14, No. 5, pp. 556-567, 1997.

12. Szente, L. and J. Szejtli, "Cyclodextrins as food ingredients", *Trends in Food Science and Technology*, Vol. 15, pp. 137-142, 2004.

13. Easton, C. J. and S. F. Lincoln, *Modified Cyclodextrins: Scaffolds and Templates for Supramolecular Chemistry*, Imperial College Press, London, 1999.

14. Hedges, A. R., "Industrial applications of cyclodextrins", *Chemical Reviews*, Vol. 98, No. 5, pp. 2035-2044, 1998.

15. Folkman, J., P. B. Weisz, M. M. Joullie, W. W. Li and W. R. Ewing, "Control of angio-genesis with synthetic heparin substitutes", *Science*, Vol. 243, No. 4897, pp. 1490-1493, 1989.

16. Anderson, S., T. D. W. Claridge and H. L. Anderson, "Azo-Dye Rotaxanes", *Angewandte Chemie International Edition*, Vol. 36, No. 12, pp. 1310-1313, 1997.

17. Craig, M. R., G. Michael, T. D. Hutchings, W. Claridge and H. L. Anderson, "Rotaxane-encapsulation enhances the stability of an azo dye, in solution and when bonded to cellulose ", *Angewandte Chemie International Edition*, Vol. 113, No. 6, pp. 1105-1108, 2001.

18. Nepogodiev, S. A. and J. F. Stoddart, "Cyclodextrin-based catenanes and rotaxanes", *Chemical Reviews*, Vol. 98, No. 5, pp. 1959-1976, 1998.

19. Harada A., "Cyclodextrin-Based Molecular Machines", *Accounts of Chemical Research*, Vol. 34, No. 6, pp. 456-464, 2001.

20. Rau, H., "Photoisomerization of azobenzenes,", *Photochemistry and Photophysics*, Vol. 2, No. 4, pp. 119-141, 1990.

21. Jiang, D. L. and T. Aida, "Photoisomerization in Dendrimers by Harvesting of Low-Energy Photons", *Nature*, Vol. 388, pp. 454– 456, 1997.

22. Wang, Y., N. Ma, Z. Wang and X. Zhang, "Photocontrolled Reversible Supramolecular Assemblies of an Azobenzene-Containing Surfactant with α-Cyclodextrin", *Angewandte Chemie International Edition*, Vol. 46, No. 16, pp. 2823 –2826, 2007.

23. Wang, Z., Z. Li and Z. Liu, "Photostimulated Reversible Attachment of Gold Nanoparticles on Multiwalled Carbon Nanotubes", *Journal of Physical Chem*istry, Vol. 113, No. 10, pp. 3899-3902, 2009.

24. Sukhorukov, G. B., A. L. Rogach, M. Garstka, S. Springer, W.J. Parak, A. Muñoz-Javier, O. Kreft, A. G. Skirtach, A. S. Susha, Y. Ramaye, R. Palankar and M. Winterhalter, "Multifunctionalized Polymer Microcapsules: Novel Tools for Biological and Pharmacological Applications", *Small*, Vol. 3, No. 6, pp. 944-955, 2007.

25. Torchilin, V. F., "Recent advances with liposomes as pharmaceutical carriers", *Nature Drug Discovery*, Vol. 4, pp. 45-160, 2005.

26. Cavalieri, F., A. Postma, L. Lee and F. Caruso, "Assembly and Functionalization of DNA-Polymer Microcapsules", *ACS Nano*, Vol. 3, No. 1, pp. 234-240, 2009.

27. Skirtach, A. G., P. Karageorgiev, M. F. Bedard, G. B. Sukhorukov and H. Möhvald, "Reversibly Permeable Nanomembranes of Polymeric Microcapsules", *Journal of American Chemical Society*, Vol. 130, No. 35, pp. 11572-11573, 2008.

28. Peyratout, C. S. and L. Dähne, "Tailor-made polyelectrolyte microcapsules: from multilayers to smart containers", *Angewandte Chemie International Edition*, Vol 43, No. 29, pp. 3762-3783, 2004.

29. Zelikin, A. N., Q. Li and F. Caruso, "Degradable Polyelectrolyte Capsules Filled with Oligonucleotide Sequences", *Angewandte Chemie International Edition*, Vol. 118, No. 46, pp. 7907-7909, 2006.

30. Symon, Z., A. Peyser, D. Tzemach, O. Lyass, E. Sucher, E. Shezen and A. Gabizon, "Selective delivery of Doxorubicin to patients with breast carcinoma metastases by stealth liposomes", *Cancer*, Vol. 86, No. 1, pp. 72-78, 1999.

31. Skirtach, A.G., A. M. Javier, O. Kreft, K. Köhler, A. P. Alberola, H. Möhwald, W. J. Parak and G. B. Sukhorukov, "Laser-Induced Release of Encapsulated Materials inside Living Cells", *Angewandte Chemie International Edition*, Vol. 45, No. 28, pp. 4612 – 4617, 2006.

32. Binder, W. H., "Supramolecular Assembly of Nanoparticles at Liquid-Liquid Interfaces", *Angewandte Chemie International Edition*, Vol. 44, No. 33, pp. 5172-5175, 2005.

33. Dinsmore, A. D., M. F. Hsu, M. G. Nikolaides, M. Marquez, A. R. Bausch and D. A. Weitz, "Colloidosomes: Selectively Permeable Capsules Composed of Colloidal Particles", *Science*, Vol. 298, No. 5595, pp. 1006-1009, 2002.

34. Boker, A., J. He, T. Emrick and T. P. Russell, "Self-assembly of nanoparticles at interfaces", *Soft Matter*, Vol. 3, pp. 1231-1248, 2007.

35. Daniel, M. and D. Astruc, "Gold nanoparticles: assembly, supramolecular chemistry, quantum-size-related properties, and applications toward biology, catalysis, and nanotechnology," *Chemical Reviews*, Vol. 104, No. 1, pp. 293-346, 2004.

36. Turkevitch, J., P. Stevenson and J. Hillier, "A Study of the Nucleation and growth process in the synthesis of colloidal gold," *Discussions Faraday Society*, Vol. 11, pp. 55-75, 1951.

37. Brust, M., M. Walker, D. Bethell, D. Schiffrin and R. Whyman, "Synthesis of thiol-derivatised gold nanoparticles in a two-phase liquid–liquid system," *Journal of the Chemical Society, Chemical Communications*, Vol. 7, No. 7, pp. 801-802, 1994.

38. Binks , B. and J. Clint, "Solid wettability from surface energy components: Relevance to Pickering emulsions," *Langmuir*, Vol. 18, No. 4, pp. 1270-1273, 2002.

39. Lin, Y., H. Skaff, T. Emrick, A. D. Dinsmore and T. P. Russell, "Nanoparticle Assembly and Transport at Liquid-Liquid Interfaces", *Science*, Vol. 299, No. 5604, pp. 226-229, 2003.

40. Binks, B. P. And T. S. Horozov, *Colloidal Particles at Liquid-Liquid Interfaces*, Cambridge University Press, 2006.

41. Bresme, F. and M. Oettel, "Nanoparticle at Fluid Interfaces", *Journal of Physics: Condensed Matter*, Vol. 19, pp. 413101–413134, 2007.

42. Lin, Y., H. Skaff, A. Boeker, A. D. Dinsmore, T. Emrick and T. P. Russell, "Ultrathin Cross-linked Nanoparticle Membranes", *Journal of American Chemical Society*, Vol. 125, No. 42, pp. 12690 –12691, 2003.

43. Samanta, B., D. Patra, C. Subramani, Y. Ofir, G. Yesilbag, A. Sanyal and V. M. Rotello, "Stable Magnetic Colloidosomes via Click-Mediated Crosslinking of Nanoparticles at Water–Oil Interfaces", *Small*, Vol. 5, No. 6, pp. 685 –688, 2009.

44. Shenhar, R. and V. M. Rotello, "Nanoparticles: Scaffolds and Building Blocks", *Accounts of Chemical Research*, Vol. 36, No. 7, pp. 549 –561, 2003.

45. Ashton, P.R., R. Koniger, J.F. Stoddart, D. Alker and V.D. Harding, "Amino Acid Derivatives of β-Cyclodextrin", *The Journal of Organic Chemistry*, Vol. 61, No. 3, pp. 903-908, 1996.

46. Rojas, M.T., R. Koeniger, J.F. Stoddart and A.E. Kaifer, "Supported Monolayer Containing Preformed Binding Sites. Synthesis and Interfacial Binding Properties of a Thiolated beta-Cyclodextrin Derivative", *Journal of the American Chemical Society*, Vol. 117, No. 1, pp. 336-343, 1995.

47. Liu, J., W. Ong, E. Roman, M.J. Lynn and A.E. Kaifer, "Cyclodextrin-Modified Gold Nanospheres", *Langmuir*, Vol. 16, No. 7, pp. 3000-3002, 2000.

48. Paau, M. C., C. K. Lo, X. Yang and M. M. F. Choi, "Synthesis of 1.4 nm α-cyclodextrin-protected gold nanoparticles for luminescence sensing mercury(II) with picomolar detection limit", *Journal of Physical Chemistry,* Vol. 114, No. 38, pp. 15995–16003, 2010.

49. Choi, M. M. F., A. D. Dougles and R. W. Murray, "Ion-Pair Chromatographic Separation of Water-Soluble Gold Monolayer-Protected Clusters", *Analytical Chemistry*, Vol. 78, No. 8, pp. 2779– 2785, 2006.

50. Lo, C. K., M. C. Paau, D. Xiao and M. M. F. Choi, "Capillary Electrophoresis, Mass Spectrometry, and UV-Visible Absorption Studies on Electrolyte-Induced Fractionation of Gold Nanoclusters", *Analytical Chemistry*, Vol. 80, No. 7, pp. 2439-2446, 2008.

51. Zhang, Y., S. Shuang, C. Dong, C. K. Lo, M. C. Paau and M. M K. Choi, "Application of HPLC and MALDI-TOF MS for Studying As-Synthesized Ligand-Protected Gold Nanoclusters Products", *Analytical Chemistry*, Vol. 81, No. 4, pp. 1676– 1685, 2009.

52. Galow, T. H., J. Rodrigo, K. Cleary, G. Cooke and V. M. Rotello, "Fluorocarbonylferrocene. A Versatile Intermediate for Ferrocene Esters and Amides", *Journal of Organic Chemistry*, Vol. 64, No. 10, pp. 3745-3746, 1999.

53. Mulder, A., T. Auletta, A. Sartori, S. Del Ciotto, A. Casnati, R. Ungaro, J. Huskens and D.N. Reinhoudt, "Divalent Binding of a Bis(adamantyl)-Functionalized Calix[4]arene to β-cyclodextrin-based Hosts: An Experimental and Theoretical Study on Multivalent Binding in Solution and at Self-Assembled Monolayers", *Journal of the American Chemical Society*, Vol. 126, No. 21, pp. 6627-6636, 2004.

54. Liu, J., S. Mendoza, E. Roman, M.J. Lynn, R. Xu and A.E. Kaifer, "Cyclodextrin-Modified Gold Nanospheres. Host−Guest Interactions at Work to Control Colloidal Properties," *Journal of the American Chemical Society*, Vol. 121, No. 17, pp. 4304-4305, 1999.